

**AFRL-PR-WP-TM-1999-XXXX**



**HIGH CYCLE FATIGUE (HCF)  
SCIENCE AND TECHNOLOGY PROGRAM  
1999 ANNUAL REPORT**

**Multiple Authors**

**Prepared by:**

**Universal Technology Corporation  
1270 North Fairfield Road  
Dayton OH 45432-2600**

**JANUARY 2000**

**FINAL REPORT FOR THE PERIOD 1/1/99 – 12/31/99**

**APPROVED FOR PUBLIC RELEASE; DISTRIBUTION UNLIMITED**

**PROPULSION DIRECTORATE  
AIR FORCE RESEARCH LABORATORY  
AIR FORCE MATERIEL COMMAND  
WRIGHT-PATTERSON AIR FORCE BASE OH 45433-7251**

# NOTICE

USING GOVERNMENT DRAWINGS, SPECIFICATIONS, OR OTHER DATA INCLUDED IN THIS DOCUMENT FOR ANY PURPOSE OTHER THAN GOVERNMENT PROCUREMENT DOES NOT IN ANY WAY OBLIGATE THE US GOVERNMENT. THE FACT THAT THE GOVERNMENT FORMULATED OR SUPPLIED THE DRAWINGS, SPECIFICATIONS, OR OTHER DATA DOES NOT LICENSE THE HOLDER OR ANY OTHER PERSON OR CORPORATION; OR CONVEY ANY RIGHTS OR PERMISSION TO MANUFACTURE, USE, OR SELL ANY PATENTED INVENTION THAT MAY RELATE TO THEM.

THIS REPORT IS RELEASABLE TO THE NATIONAL TECHNICAL INFORMATION SERVICE (NTIS). AT NTIS, IT WILL BE AVAILABLE TO THE GENERAL PUBLIC, INCLUDING FOREIGN NATIONS.

THIS TECHNICAL REPORT HAS BEEN REVIEWED AND IS APPROVED FOR PUBLICATION.

---

Daniel E. Thomson, AFRL/PRTC

---

Theodore G. Fecke, AFRL/PRTC

---

Richard J. Hill, AFRL/PRT

IF YOUR ADDRESS HAS CHANGED, IF YOU WISH TO BE REMOVED FROM OUR MAILING LIST, OR IF THE ADDRESSEE IS NO LONGER EMPLOYED BY YOUR ORGANIZATION PLEASE NOTIFY AFRL/PRT, WRIGHT-PATTERSON AFB OH 45433-7251 TO HELP MAINTAIN A CURRENT MAILING LIST.

Do not return copies of this report unless contractual obligations or notice on a specific document requires its return.

REPORT DOCUMENTATION PAGE			Form Approved OMB No. 074-0188	
Public reporting burden for this collection of information is estimated to average 1 hour per response, including the time for reviewing instructions, searching existing data sources, gathering and maintaining the data needed, and completing and reviewing this collection of information. Send comments regarding this burden estimate or any other aspect of this collection of information, including suggestions for reducing this burden to Washington Headquarters Services, Directorate for Information Operations and Reports, 1215 Jefferson Davis Highway, Suite 1204, Arlington, VA 22202-4302, and to the Office of Management and Budget, Paperwork Reduction Project (0704-0188), Washington, DC 20503				
1. AGENCY USE ONLY (Leave blank)	2. REPORT DATE January 2000	3. REPORT TYPE AND DATES COVERED 1999 Annual Report (1 Jan – 31 Dec 99)		
4. TITLE AND SUBTITLE High Cycle Fatigue (HCF) Science and Technology Program 1998 Annual Report		5. FUNDING NUMBERS C – F33615-98-C-2807 PE – 62203F PR – 3066		
6. AUTHOR(S) various		TA – 14 WU – 20		
7. PERFORMING ORGANIZATION NAME(S) AND ADDRESS(ES)  Propulsion Directorate Air Force Research Laboratory Air Force Materiel Command Wright-Patterson Air Force Base, OH 45433-7251		8. PERFORMING ORGANIZATION REPORT NUMBER  Universal Technology Corporation 1270 N. Fairfield Rd. Dayton, OH 45432-2600		
9. SPONSORING / MONITORING AGENCY NAME(S) AND ADDRESS(ES)  Propulsion Directorate Air Force Research Laboratory Air Force Materiel Command Wright-Patterson Air Force Base, OH 45433-7251		10. SPONSORING / MONITORING AGENCY REPORT NUMBER AFRL-PR-WP-____-____  POC: Daniel E. Thomson AFRL/PRTC 937-255-2081		
11. SUPPLEMENTARY NOTES				
12a. DISTRIBUTION / AVAILABILITY STATEMENT Approved for Public Release; Distribution Unlimited			12b. DISTRIBUTION CODE	
13. ABSTRACT (Maximum 200 Words) This third annual report of the National Turbine Engine High Cycle Fatigue (HCF) Program is a brief review of work completed, work in progress, and technical accomplishments. This program is a coordinated effort with participation by the Air Force, the Navy, and NASA. The technical efforts are organized under eight Action Teams including: Materials Damage Tolerance Research, Forced Response Prediction, Component Analysis, Instrumentation, Passive Damping Technology, Component Surface Treatments, Aeromechanical Characterization, and Engine Demonstration. Daniel E. Thomson, AFRL/PRTC, Wright-Patterson AFB, is the Program Manager.				
14. SUBJECT TERMS High Cycle Fatigue, Turbine Engines, Instrumentation, Damping, Forced Response, Aeromechanical Characterization, Materials, Surface Treatments, Laser Shock Peening, Component Analysis, Damage Tolerance			15. NUMBER OF PAGES	
			16. PRICE CODE	
17. SECURITY CLASSIFICATION OF REPORT	18. SECURITY CLASSIFICATION OF THIS PAGE Unclassified	19. SECURITY CLASSIFICATION OF ABSTRACT Unclassified	20. LIMITATION OF ABSTRACT	

NSN 7540-01-280-5500

Standard Form 298 (Rev. 2-89)  
Prescribed by ANSI Std. Z39-18  
298-102



## **TABLE OF CONTENTS**

	<b><u>Page</u></b>
<b>1.0 COMPONENT SURFACE TREATMENTS .....</b>	<b>1</b>
1.1 <i>Laser Shock Peening (LSP) vs. Shot Peening Competition .....</i>	<i>3</i>
1.2 <i>Laser Optimization Development .....</i>	<i>5</i>
1.3 <i>Production LSP Facility Development .....</i>	<i>6</i>
1.4 <i>LSP Process Modeling.....</i>	<i>7</i>
1.5 <i>RapidCoater<sup>®</sup> for LSP .....</i>	<i>9</i>
1.5.1 <i>Rapid Overlay Concept Development.....</i>	<i>9</i>
1.5.2 <i>Development of a RapidCoater<sup>®</sup> Manufacturing System .....</i>	<i>9</i>
1.6 <i>Manufacturing Technology for Affordable LSP .....</i>	<i>11</i>
1.7 <i>Conclusion .....</i>	<i>12</i>
<b>2.0 MATERIALS DAMAGE TOLERANCE RESEARCH.....</b>	<b>13</b>
2.1 <i>Microstructure Effects of Titanium HCF (Fan).....</i>	<i>15</i>
2.2 <i>Air Force In-House Research (Fan &amp; Turbine) .....</i>	<i>17</i>
2.3 <i>HCF and Time-Dependent Failure in Metallic Alloys for Propulsion Systems               (Fan &amp; Turbine).....</i>	<i>23</i>
2.4 <i>Improved HCF Life Prediction (Fan).....</i>	<i>28</i>
2.5 <i>Advanced HCF Life Assurance Methodologies (Fan &amp; Turbine) .....</i>	<i>34</i>
2.6 <i>Conclusion .....</i>	<i>35</i>
<b>3.0 INSTRUMENTATION.....</b>	<b>36</b>
3.1 <i>Improved Non-Interference Stress Measurement System (NSMS).....</i>	<i>39</i>
3.1.1 <i>Improved NSMS Hardware (Generation 4).....</i>	<i>39</i>
3.1.2 <i>Alternate Tip Sensors.....</i>	<i>44</i>
3.1.3 <i>Enhanced NSMS Data Processing Capability for Generation 4 &amp; 5 NSMS               Development) .....</i>	<i>44</i>
3.1.4 <i>Spin Pit Validation of NSMS .....</i>	<i>45</i>
3.1.5 <i>High Temperature NSMS Sensor Development.....</i>	<i>46</i>
3.2 <i>Environmental Mapping System .....</i>	<i>47</i>
3.2.1 <i>Pressure/Temperature Sensitive Paint (PSP/TSP) .....</i>	<i>47</i>
3.2.1.1 <i>PSP: Improved Dynamic Response .....</i>	<i>48</i>
3.2.1.2 <i>PSP: Light Emitting Diodes (LEDs).....</i>	<i>50</i>

## **TABLE OF CONTENTS (Cont'd)**

	<b><u>Page</u></b>
3.2.2 <i>Comparison Testing / Air Etalons .....</i>	51
3.2.3 <i>Thin-Film Garnet.....</i>	52
3.2.4 <i>High and Low Temperature Validation of Paint/Optical Pressure Mapping .....</i>	53
3.3 <i>Improved Conventional Sensors .....</i>	53
3.3.1 <i>Non-Optical NSMS Sensor Development (Eddy Current) .....</i>	53
3.4 <i>Development of Long-Life, Less Intrusive Gages.....</i>	56
3.4.1 <i>Advanced Thin-Film Dynamic Gages.....</i>	56
3.4.2 <i>Advanced High-Temperature Thin-Film Dynamic Gages.....</i>	57
3.4.3 <i>Spin Pit Validation of Strain Gages &amp; Spin Pit Validation of High Temperature Strain Gages.....</i>	57
3.5 <i>Conclusion .....</i>	57
<b>4.0 COMPONENT ANALYSIS.....</b>	<b>58</b>
4.1 <i>Assessment of Turbine Engine Components .....</i>	60
4.2 <i>Probabilistic Design for Turbine Engine Airfoils .....</i>	61
4.3 <i>Probabilistic Blade Design System.....</i>	63
4.4 <i>Efficient Probabilistic Analysis Methods for Turbine Engine Components .....</i>	64
4.5 <i>Conclusion .....</i>	64
<b>5.0 FORCED RESPONSE PREDICTION .....</b>	<b>65</b>
5.1 <i>Development of Physical Understanding and Models.....</i>	68
5.1.1 <i>Development of TURBO-AE .....</i>	68
5.1.2 <i>Nonlinear Modeling of Stall/Flutter .....</i>	69
5.1.3 <i>Forced Response: Mistuned Bladed Disks (REDUCE Code).....</i>	70
5.1.4 <i>Design Guidelines for Mistuned Bladed Disks (REDUCE Code) .....</i>	70
5.1.5 <i>Tip Modes in Low-Aspect-Ratio Blading.....</i>	71
5.1.6 <i>Development of Aeroelastic Capability for the TURBO Code .....</i>	72
5.1.7 <i>Dynamic Analysis &amp; Design of Shroud Contact.....</i>	73
5.1.8 <i>Friction Damping in Bladed Disks .....</i>	73
5.2 <i>Acquisition of Experimental Data .....</i>	74
5.2.1 <i>High Mach Forcing Functions .....</i>	74

## **TABLE OF CONTENTS (Cont'd)**

	<b><u>Page</u></b>
5.2.2 <i>Forward Swept Blade Aeromechanics</i> .....	76
5.2.3 <i>Oscillating Cascade Rig</i> .....	77
5.2.4 <i>F109 Unsteady Stator Loading</i> .....	78
5.2.5 <i>Fluid-Structure Interaction</i> .....	80
5.2.6 <i>Experimental Study of Forced Response in Turbine</i> .....	81
5.3 <i>Validation of Analytical Models</i> .....	82
5.3.1 <i>Evaluation of Current State-of-the-Art Unsteady Aerodynamic Models for the Prediction of Flutter &amp; Forced Vibration Response</i> .....	82
5.3.2 <i>Evaluation of State-of-the-Art Aerodynamic Models</i> .....	83
5.3.3 <i>Forced Response Prediction System (Fans)</i> .....	84
5.3.4 <i>Aeromechanical Design System Validation</i> .....	85
5.3.5 <i>Probabilistic Structural Analysis Methods</i> .....	85
5.4 <i>Conclusion</i> .....	86
<b>6.0 PASSIVE DAMPING TECHNOLOGY</b> .....	<b>87</b>
6.1 <i>Identification &amp; Characterization of Damping Techniques</i> .....	89
6.1.1 <i>Mechanical Damping Concepts</i> .....	89
6.1.2 <i>Air Force In-House Damping Investigations</i> .....	90
6.1.3 <i>Centrifugally Loaded Viscoelastic Material Characterization Testing</i> .....	95
6.1.4 <i>Damping for Extreme Environments</i> .....	98
6.1.5 <i>Centrifugally Loaded Particle Damping</i> .....	101
6.2 <i>Modeling and Incorporation of Damping in Components</i> .....	103
6.2.1 <i>Advanced Damping Concepts for Reduced HCF</i> .....	103
6.2.2 <i>Damping Systems for the Integrated High Performance Turbine Engine Technology (IHPTET) Program</i> .....	105
6.2.3 <i>Evaluation of Reinforced Swept Airfoils / Internal Dampers</i> .....	107
6.2.4 <i>Damping for Turbines</i> .....	108
6.2.5 <i>Dual Use Program</i> .....	109
6.2.6 <i>Transition of Damping Technology to counterrotating Low Pressure Turbine Blades</i> .....	109

## **TABLE OF CONTENTS (Cont'd)**

	<b><u>Page</u></b>
6.3 <i>Conclusion</i> .....	110
<b>7.0 AEROMECHANICAL CHARACTERIZATION</b> .....	111
7.1 <i>Compressor Mistuning Characterization</i> .....	113
7.2 <i>Fretting Characterization</i> .....	114
7.3 <i>Spin Pit Excitation Methods</i> .....	115
7.4 <i>Compressor Blade Fracture &amp; Fatigue Evaluation</i> .....	116
7.5 <i>Rotational Validation of Mistuning Model</i> .....	117
7.6 <i>Development of Multi-Axial Fatigue Testing Capability</i> .....	118
7.7 <i>Inlet Distortion Characterization</i> .....	120
7.8 <i>Engine Structural Integrity Program (ENSIP) / Joint Service Specification Guide (JSSG)</i> .....	122
7.9 <i>Conclusion</i> .....	123
<b>8.0 ENGINE DEMONSTRATION</b> .....	124
8.1 <i>General Electric / Allison Advanced Development Company</i> .....	127
8.1.1 <i>XTC76/2</i> .....	127
8.1.2 <i>XTC76/3</i> .....	128
8.1.3 <i>XTC77/SE</i> .....	129
8.1.4 <i>XTE76/1</i> .....	130
8.1.5 <i>XTC77</i> .....	131
8.2 <i>Pratt &amp; Whitney</i> .....	133
8.2.1 <i>XTE66/A1</i> .....	133
8.2.2 <i>XTC66/SC</i> .....	134
8.2.3 <i>XTC66/1B</i> .....	135
8.2.4 <i>XTE66/1</i> .....	136
8.2.5 <i>XTC67/1</i> .....	137
8.2.6 <i>XTE66/SE</i> .....	138
8.2.7 <i>XTE67/1</i> .....	139
8.2.8 <i>XTE65/3</i> .....	140
8.3 <i>Conclusion</i> .....	141

## LIST OF FIGURES

	<u>Page</u>
<b>FIGURE 1</b>	<i>HCF Team Organizational Structure</i> .....xi
<b>FIGURE 2</b>	<i>Damage Tolerance Data for LSP'd Blades</i> .....3
<b>FIGURE 3</b>	<i>What Is Laser Shock Peening?</i> .....4
<b>FIGURE 4</b>	<i>Peak Rise Time Before &amp; After Laser System Modifications</i> .....5
<b>FIGURE 5</b>	<i>Schematic of Laser System Operations</i> .....6
<b>FIGURE 6</b>	<i>Comparison of Modeled and Experimental Residual Stresses for Estimated Similar Pressure Conditions</i> .....8
<b>FIGURE 7</b>	<i>Interrelationship between LSP Programs</i> .....10
<b>FIGURE 8</b>	<i>S-N Input Data and Fatigue Strength Model Results for Bimodal Fine Uni-Rolled, Bimodal Forged, and Equiaxed Forged Microstructures</i> .....16
<b>FIGURE 9</b>	<i>Pre-Crack &amp; Step-Test Loading Technique Used to Determine LCF/HCF Thresholds</i> .....18
<b>FIGURE 10</b>	<i>LCF/HCF Thresholds for HCF Stress Ratio <math>R=0.1</math></i> .....18
<b>FIGURE 11</b>	<i>Residual Stress vs. Depth for Five Shocks per Spot</i> .....21
<b>FIGURE 12</b>	<i>Comparison of Pre-Strained and “As Received” Material Fatigue Limit Stress at <math>10^7</math> Cycles</i> .....22
<b>FIGURE 13</b>	<i>New HCF/LCF Fretting Fatigue Test Apparatus</i> .....23
<b>FIGURE 14</b>	<i>Constant-<math>K_{max}</math> Fatigue Crack Propagation Behavior</i> .....25
<b>FIGURE 15</b>	<i>Comparison of Long-Crack Propagation Data to Fatigue Data from Small Cracks</i> .....25
<b>FIGURE 16</b>	<i>Scanning Electron Microscope Micrographs of Impact Damage Sites for a 300 m/s Impact Velocity</i> .....26
<b>FIGURE 17</b>	<i>Scanning Electron Microscope Micrographs Showing the Presence of Microcracking at Crater Rim of FOD Indent</i> .....26
<b>FIGURE 18</b>	<i>Fatigue Crack Propagation Rate of Naturally-Initiated “Small” Cracks</i> .....29
<b>FIGURE 19</b>	<i>Representative FOD from Ballistic and Solenoid Gun Impacts</i> .....31
<b>FIGURE 20</b>	<i>Evolution of Coefficient of Friction</i> .....32
<b>FIGURE 21</b>	<i>Comparison of Surface Normal Traction Obtained from Integral Equation and FEM Methods</i> .....33
<b>FIGURE 22</b>	<i>Materials Damage Tolerance Damage State Exit Criteria</i> .....34

## LIST OF FIGURES

	<u>Page</u>
<b>FIGURE 23</b> <i>Next-Generation NSMS Overview .....</i>	39
<b>FIGURE 24</b> <i>Five-Lens Line Probe .....</i>	41
<b>FIGURE 25</b> <i>F100-220 First-Stage High Compressor NSMS Flight Probe .....</i>	42
<b>FIGURE 26</b> <i>F100-220 First-Stage High Compressor NSMS Optical Probe Lead Routing.....</i>	42
<b>FIGURE 27</b> <i>PSP Test Setup .....</i>	47
<b>FIGURE 28</b> <i>PSP Response to a 0.2-psi Pressure Modulation at 5.7 kHz .....</i>	49
<b>FIGURE 29</b> <i>Eddy Current Sensor Vibration Estimate, SFET#1, Blade 10, 2<sup>nd</sup> Torsion Mode .....</i>	54
<b>FIGURE 30</b> <i>Eddy Current Sensor Clearance Closedown, SFET#1 .....</i>	54
<b>FIGURE 31</b> <i>Eddy Current Sensor Foreign Object Detection, SFET#1 Composite Material (10mm x 10mm x 3mm) .....</i>	55
<b>FIGURE 32</b> <i>Finite Element Model of a Joint between Two Compressor Stages .....</i>	60
<b>FIGURE 33</b> <i>Probabilistic HCF Prediction System .....</i>	62
<b>FIGURE 34</b> <i>Purdue High Speed Compressor Configuration.....</i>	74
<b>FIGURE 35</b> <i>Schematic of F109 Engine Showing Location of Pressure-Instrumented Stators.....</i>	79
<b>FIGURE 36</b> <i>Dynamic Spin Facility, NASA Glenn Research Center .....</i>	90
<b>FIGURE 37</b> <i>Model Fan Test Article .....</i>	91
<b>FIGURE 38</b> <i>The Electrical Connections between Piezoelectric Actuators .....</i>	92
<b>FIGURE 39</b> <i>Extended Mode Shapes for Eight Blades.....</i>	92
<b>FIGURE 40</b> <i>Mode Shapes for the Mistuned, Uncoupled Case .....</i>	93
<b>FIGURE 41</b> <i>Mode Shapes for the Mistuned, Coupled Case .....</i>	93
<b>FIGURE 42</b> <i>Mode Shapes for the Tuned, Uncoupled Case .....</i>	94
<b>FIGURE 43</b> <i>Mode Shapes for the Tuned, Coupled Case.....</i>	94
<b>FIGURE 44</b> <i>Viscoelastic Tub Blade Hardware .....</i>	95
<b>FIGURE 45</b> <i>Damping Study Blade .....</i>	96
<b>FIGURE 46</b> <i>Comparison of Measured and Predicted Static Strain .....</i>	96
<b>FIGURE 47</b> <i>Comparison of Undamped and Damped Blade Response (One Pocket) to PZT Excitation in the Laboratory.....</i>	97
<b>FIGURE 48</b> <i>Selected Frames from Particle Damper Simulation .....</i>	99

## LIST OF FIGURES

	<u>Page</u>
<b>FIGURE 49</b> <i>Undamped to Damped Comparison for Single and Multiple-Particle Tests .....</i>	100
<b>FIGURE 50</b> <i>High-Temperature Test Articles .....</i>	100
<b>FIGURE 51</b> <i>Example Time Domain Ring Down and Extracted Hilbert Transform Profile with Linear Fits for a Baseline Non Damped Test Object .....</i>	102
<b>FIGURE 52</b> <i>Phase II Blade, Counterbalance, and Test Capsules Prior To Blade Wiring and Encapsulation .....</i>	102
<b>FIGURE 53</b> <i>Delphi Analysis of Damping Concepts .....</i>	104
<b>FIGURE 54</b> <i>Damped ACCS Blisk .....</i>	106
<b>FIGURE 55</b> <i>Weld Failure .....</i>	106
<b>FIGURE 56</b> <i>2B/1T Mode Interaction.....</i>	113
<b>FIGURE 57</b> <i>Mistuning Validation Simulated Bladed Disk.....</i>	117
<b>FIGURE 58</b> <i>Proof of Concept Biaxial Fatigue Fixture .....</i>	118
<b>FIGURE 59</b> <i>Multi-Axial Fatigue Model .....</i>	119
<b>FIGURE 60</b> <i>Initial Correlation between Vibratory Stresses and Model Excitation Index.....</i>	119
<b>FIGURE 61</b> <i>CFD Prediction and Measurements of 3/rev of Supersonic, Decel.....</i>	119
<b>FIGURE 62</b> <i>Modified Correlation between Vibratory Stresses and MEI .....</i>	119

## **FOREWORD**

This document, the third annual report of the National Turbine Engine High Cycle Fatigue (HCF) Science and Technology (S&T) Program, is a summary of the objectives, approaches, and technical progress of ongoing and planned future efforts.

High cycle fatigue (HCF) results from vibratory stress cycles induced from various aeromechanical sources. The frequencies can be thousands of cycles per second. HCF is a widespread phenomenon in aircraft gas turbine engines that historically has led to the premature failure of major engine components (fans, compressors, turbines) and in some instances has resulted in loss of the total engine and aircraft.

Between 1982 and 1996, high cycle fatigue accounted for 56% of Class A engine-related failures. HCF is a major factor negatively impacting safety, operability, and readiness, while at the same time increasing maintenance costs. In fiscal year 1994, HCF required an expenditure of 850,000 maintenance man-hours for risk management inspections. Estimates put the cost of high cycle fatigue at over \$400 million per year.

The National HCF S&T Program officially began in December 1994. The purpose of this national effort was to help eliminate HCF as a major cause of engine failures. The Program is directed by an Air Force led steering committee consisting of representatives from the Air Force, the Navy, and NASA, along with an adjunct industry advisory panel. The Organizational Structure of the HCF Team is shown below.

The HCF S&T Program is specifically directed at supporting the Integrated High Performance Turbine Engine Technology (IHPTET) Program, and one of its goals: to reduce engine maintenance costs. This program will try to achieve that goal through technical action team efforts targeted at a 50% reduction of HCF-related maintenance costs. In addition, the program could contribute to a reduction in HCF-related “real” development costs of over 50%. When combined with the Test and Evaluation (T&E) program, and future health monitoring approaches, the HCF S&T program should ensure the production of much more damage-tolerant high-performance engines.

The specific component objectives of the HCF S&T program are listed below:

	<b><u>Fans</u></b>	<b><u>Compressors</u></b>	<b><u>Turbines</u></b>
Determine Alternating Stress Within...	20%	25%	25%
Damp Resonant Stress By...	60%	20%	25%
Reduce Uncertainty in Capability of Damaged Components by...	50%	50%	50%
Increase Leading Edge Defect Tolerance...	15x (5-75 mils)	n/a	n/a

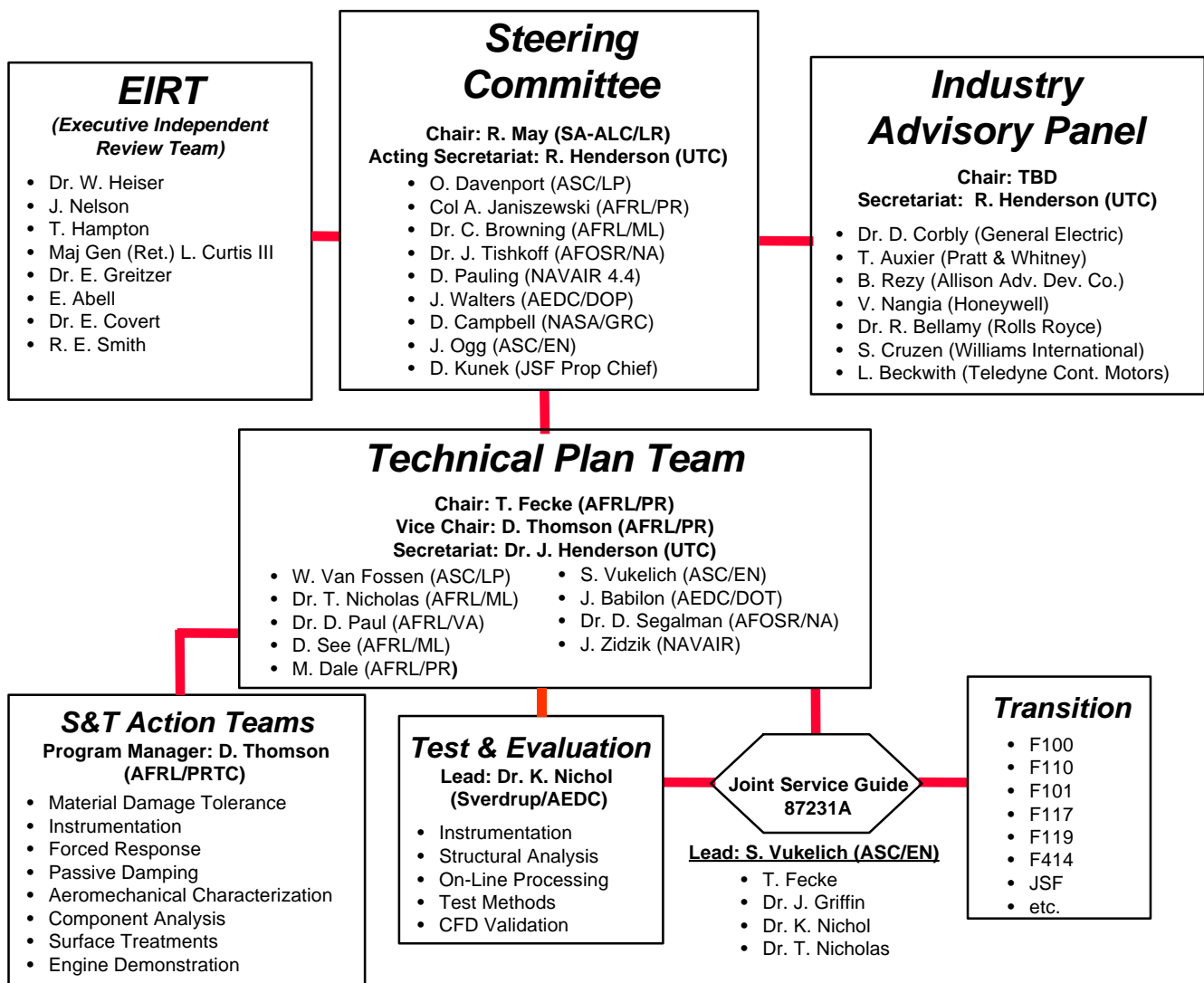


**FIGURE 1. HCF Team Organizational Structure**

The technical efforts are organized under eight action teams:

- Component Surface Treatments
- Materials Damage Tolerance Research
- Instrumentation
- Component Analysis
- Forced Response Prediction
- Passive Damping
- Aeromechanical Characterization
- Engine Demonstration (added in 1999)

Over the last several years, the technologies developed under the High Cycle Fatigue (HCF) Science and Technology (S&T) Program have helped solve several difficult field engine programs. As a result, we are now seeing considerably fewer major HCF events.

Today, excellent progress in the HCF program continues. For the first time, it appears that this once-arcane topic is being managed to a point where significant cost reductions are being realized, positively impacting the operations, maintenance, and readiness of our combat forces. However, HCF is a very difficult technology challenge that has continued to evolve multiple technology development and transition risks. During the fall of 1999 the HCF National Action Team completed a Project “Relook” study defining the efforts necessary to mitigate these critical risk issues, both current program “shortfalls” and “new requirements.” Reprogramming options have been reviewed with the HCF Steering Committee, the Industry Advisory Panel, and a special Executive Independent Review Team (EIRT) (see Fig. 1), and implementation plans are being finalized.

In the future, the HCF S&T Program will continue as a very high priority national effort. Meeting the total technology challenge could essentially eliminate engine HCF-related aircraft mishaps and greatly enhance overall aircraft systems readiness.

Your comments regarding the work reported in this document are welcome, and may be directed to Mr. Brian Garrison of Universal Technology Corporation (brian.garrison@wpafb.af.mil, 937-255-5003), or Mr. Daniel Thomson, the HCF Program Manager, of the Air Force Research Laboratory, Propulsion Directorate (AFRL/PRTC, Daniel.Thomson@wpafb.af.mil, 937-255-2081).

# 1.0 COMPONENT SURFACE TREATMENTS



## BACKGROUND

The Component Surface Treatments Action Team (Surface Treatments AT) has the responsibility of fostering collaboration between individual HCF surface treatment efforts with the goal of increasing leading edge defect tolerance by 15x (5 mils to 75 mils). The Surface Treatments AT provides technical coordination and communication between active participants involved in Laser Shock Peening (LSP) and related technologies. Annual technical workshops have been organized and summaries of these workshops are disseminated to appropriate individuals and organizations. The Chair, Co-Chair, and selected Surface Treatments AT members meet as required (estimated quarterly) to review technical activities, develop specific goals for LSP programs, and coordinate with the Technical Plan Team (TPT) and Industry Advisory Panel (IAP). The Chairman (or Co-Chair) of the Surface Treatments AT keeps the TPT Secretary informed of AT activities on a frequent (at least monthly) basis. This AT includes members from government agencies, industry, and universities who are actively involved in surface treatment technologies applicable to engine HCF. The team is to be multidisciplinary with representatives from multiple organizations representing several component technologies as appropriate. The actual membership of the AT may change in time as individuals assume different roles in related projects.

## ACTION TEAM CHAIRS



### Chair

Mr. David W. See  
U.S. Air Force  
AFRL/MLMP, Bldg. 653  
2977 P Street, Suite 6  
Wright-Patterson AFB, OH 45433-7739  
Phone: (937) 904-4387  
Fax: (937) 656-4420  
Email: David.See@afrl.af.mil



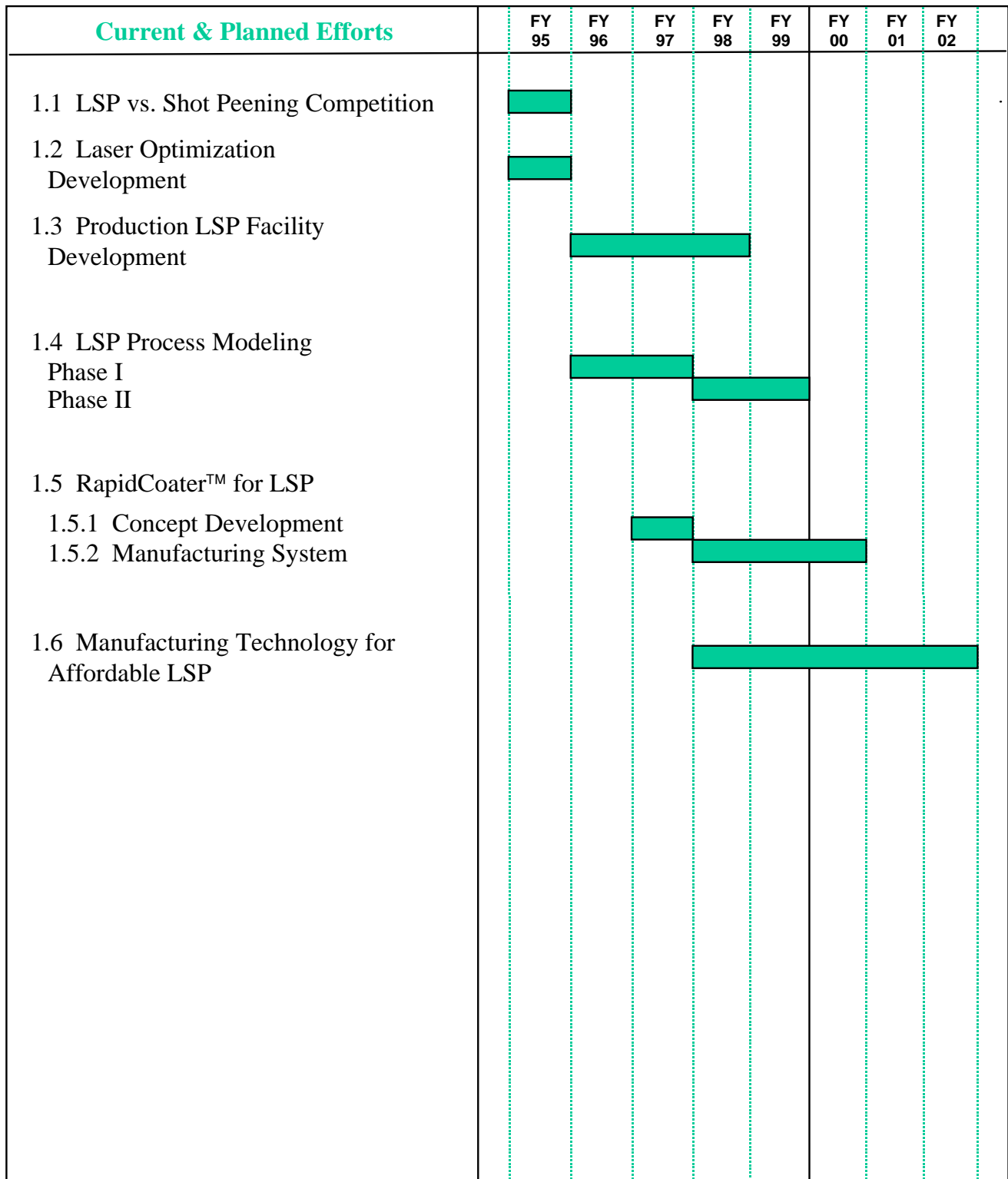
### Co-Chair

Mr. Paul R. Smith  
U.S. Air Force  
AFRL/MLLM, Bldg. 655  
2230 Tenth St., Suite 1  
Wright-Patterson AFB, OH 45433-7817  
Phone: (937) 255-1384  
Fax: (937) 255-3007  
Email: Paul.Smith@afrl.af.mil

## INTRODUCTION

The following pages summarize the schedules, backgrounds, and recent progress of the current and planned projects managed by this action team.

# Component Surface Treatments Schedule



## 1.1 Laser Shock Peening (LSP) vs. Shot Peening Competition

*FY 95*

**Background and Final Results:** In September 1995, a comparative study between a new surface treatment technology called “Laser Shock Peening” (LSP), and an established surface treatment technology called “shot peening,” was conducted. This study evaluated the damage tolerance improvements produced by these processes, specifically rating their influence for enhancing the fatigue life of turbine engine fan blades damaged by foreign objects (FOD). Critical blade characteristics, such as surface finish, change in aerodynamic profile, and manufacturability, were factored into the evaluation. The test matrix was configured to make the assessment as realistic and objective as possible. The resulting data showed that *damaged* Laser Shock Peened F101 fan blades with a 250-mil notch actually demonstrated *greater* fatigue strength than the baseline *undamaged* untreated fan blades (Fig. 2). Figure 3 describes the Laser Shock Peening process in more detail.

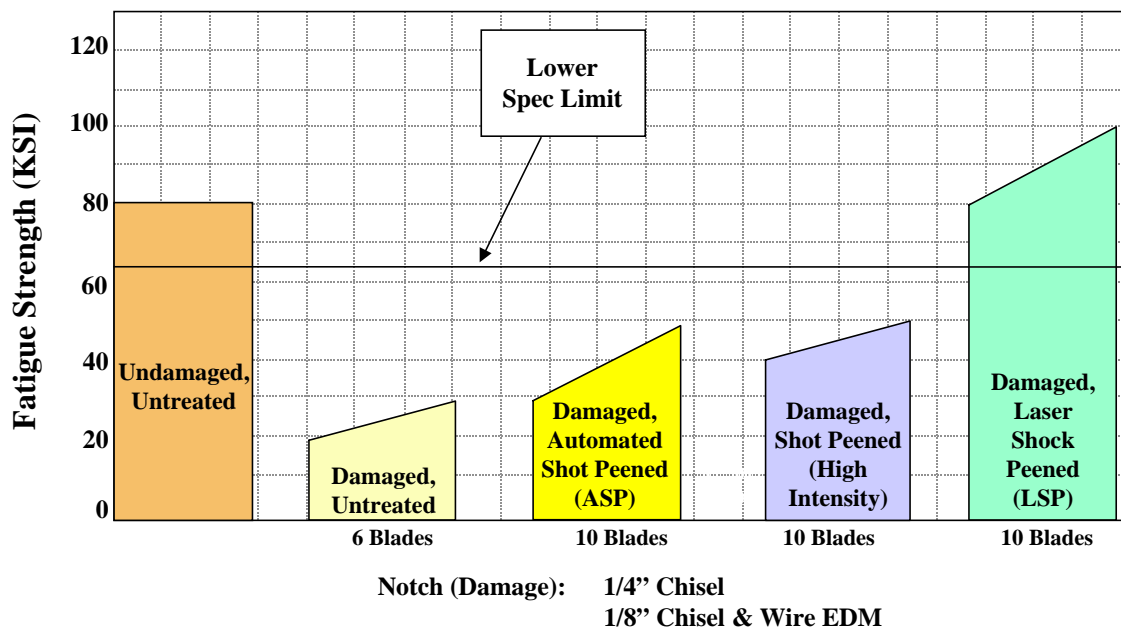


**FIGURE 2.** Damage Tolerance Data Indicating That Fatigue Strength of LSP'd Blades Is Equal to or Better Than That of Undamaged, Untreated Blades

**Participating Organizations:** GRC International, Inc.

**Points of Contact:**

Government

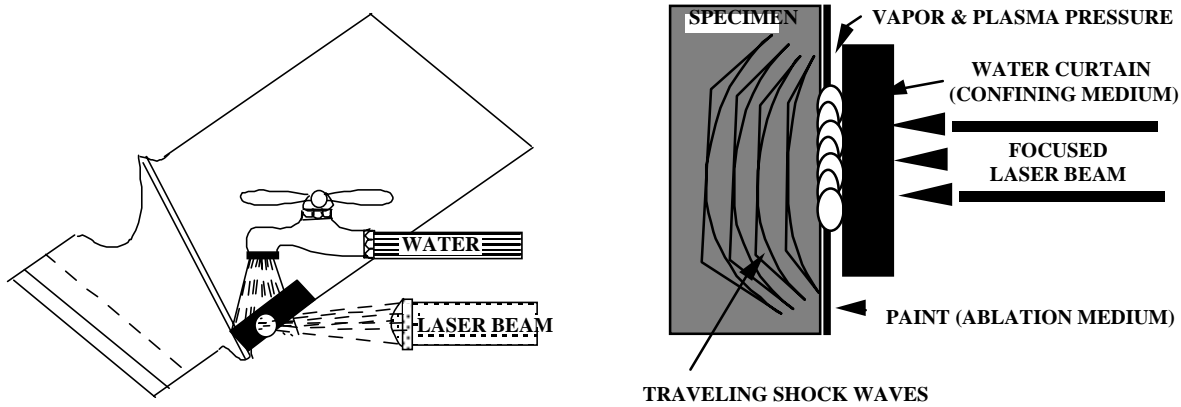
Mr. David W. See  
U.S. Air Force  
AFRL/MLMP, Bldg. 653  
2977 P Street, Suite 6  
Wright-Patterson AFB, OH 45433-7739  
Phone: (937) 255-3612  
Fax: (937) 656-4420  
Email: David.See@afri.af.mil

Contractor

Mr. Paul Sampson  
GRC International, Inc.  
2940 Presidential Dr., Suite 390  
Fairborn, OH 45424-6223  
Phone: (937) 429-7773  
Fax: (937) 429-7769  
Email: psampson@grci.com

# What Is Laser Shock Peening?

- A high energy laser pulse strikes a coated surface covered by a layer of water, causing a localized high pressure energy wave.



- A repetitive pattern of laser pulses results in an area of deep compressive stress.
- Results of industry and government testing have indicated the ability to stop crack initiation and propagation.

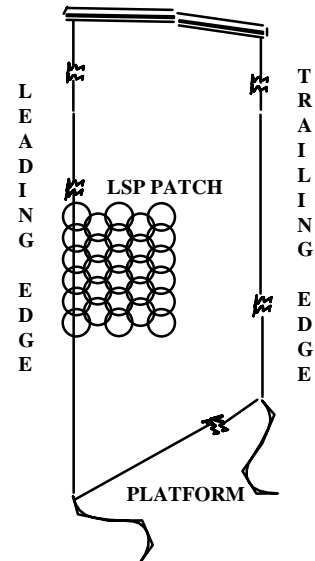


**FIGURE 3.** What Is Laser Shock Peening?

## 1.2 Laser Optimization Development

*FY 95*

**Background:** The primary objective of this program was to demonstrate the effectiveness of laser peening with elliptical and circular spots in terms of its ability to increase the fatigue life of an airfoil. A secondary objective was to demonstrate the ability to sharpen the rise time of the laser pulse using an optical switch, rather than using the traditional aluminum blow-off foil.

**Final Results:** Airfoil-shaped test specimens were laser peened using elliptical spots and circular spots and fatigue tested by the Air Force. A study of the rise time of the temporal laser pulse was conducted to confirm that an optical switch could modify the rise time of the laser pulse as effectively as an aluminum blow-off foil. An aluminum blow-off foil has traditionally been used to sharpen the leading edge of the laser pulse. A sharp rise time is important for many LSP conditions because it increases the peak pressure of the shock wave. Both elliptical and circular spots showed significant increases in fatigue life. A rise time comparable to the rise time generated with an aluminum blow-off foil was demonstrated (Fig. 4). Using the optical switch would eliminate concerns over the presence of aluminum vapor produced by the aluminum blow-off foil and the associated risks involving the health of personal and optical-component damage. It also increases the repeatability of the process.

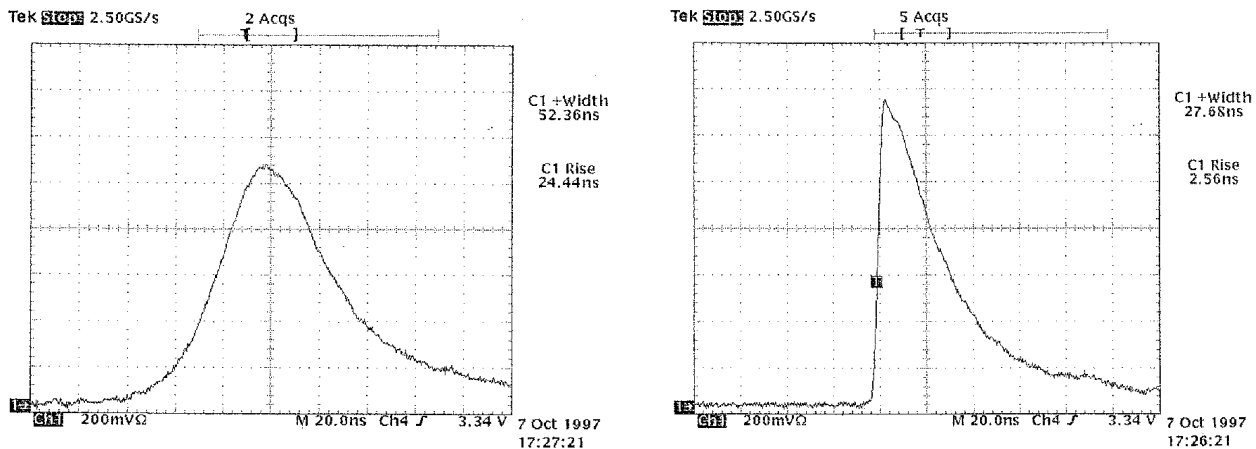


**FIGURE 4. Peak Rise Time Before & After Laser System Modifications**

**Participating Organizations:** LSP Technologies, Inc.

**Points of Contact:**

Government

Mr. David W. See  
U.S. Air Force  
AFRL/MLMP, Bldg. 653  
2977 P Street, Suite 6  
Wright-Patterson AFB, OH 45433-7739  
Phone: (937) 255-3612  
Fax: (937) 656-4420  
Email: David.See@afri.af.mil

Contractor

Dr. Jeff L. Dulaney  
LSP Technologies, Inc.  
6145 Scherers Place  
Dublin, OH 43016-1272  
Phone: (614) 718-3000 x11  
Fax: (614) 718-3007  
Email: jeff.dulaney-lspt@worldnet.att.net

## 1.3 Production LSP Facility Development

*FY 96-98*

**Background:** The primary objective of this program was to design and develop a Prototype Production Laser (PPL) capable of low levels of production. There were no commercially available lasers capable of meeting the requirements of the laser peening process. The program had three phases:

Phase I: Using working laboratory prototype lasers for the baseline design, the design was reviewed, outstanding technical issues related to the design were resolved, and the laser design was finalized. Specific technical issues to be resolved included:

1. The optical layout of the laser.
2. What system diagnostics would be used.
3. The mechanical design for the laser enclosure and electrical cabinets.

Phase II: Component acquisition, assembly, and subsystem checkout were accomplished during Phase II.

Phase III: Final laser system checkout and demonstration were accomplished in Phase III.

**Final Results:** The system, consisting of the laser, the facility, and the process (Fig. 5) was successfully demonstrated in January 1998, and the laser is now available for use by the Air Force and industry.

**FIGURE 5.** Schematic of Laser System Operations

**Participating Organizations:** GRC International, Inc.

**Points of Contact:**

Government

Mr. David W. See  
U.S. Air Force  
AFRL/MLMP, Bldg. 653  
2977 P Street, Suite 6  
Wright-Patterson AFB, OH 45433-7739  
Phone: (937) 255-3612  
Fax: (937) 656-4420  
Email: David.See@afrl.af.mil

Contractor

Mr. Paul Sampson  
GRC International, Inc.  
2940 Presidential Dr., Suite 390  
Fairborn, OH 45424-6223  
Phone: (937) 429-7773  
Fax: (937) 429-7769  
Email: psampson@grci.com

## **1.4 LSP Process Modeling**

***FY 96-99***

**Background:** In Phase I (FY 96-97) of this two-phase program, it was demonstrated that a residual stress profile could be modeled for a single laser spot. The objectives of Phase II (FY 98-99) are (1) to develop models for predicting the in-material residual stress profiles produced by multiple-spot Laser Shock Peening, (2) to verify and validate the residual stress profiles by comparison to experimental measurements, and (3) to gather appropriate data for input to the models.

A model for large-section thicknesses laser shock peened from one side has been developed and shows good correlation with experimental residual stress profiles. The correlation between the modeled and measured residual stress profiles for two different laser peening intensities (peak pressures on the metal surface) is shown in Figure 6. The thin and intermediate section thicknesses are being modeled with two-sided laser peening. This is a much more difficult problem, and several constitutive equations for the material of interest are being explored and tested with the models.

**Recent Progress:** Modeling of thick sections laser peened from one side was successful. Figure 6 shows the residual stress profiles compared to experimental profiles at two different laser peening intensities. Model verification was based on the comparison of residual stress measurements performed on LSP'd coupons with those predicted by the model. The residual stress profiles developed in a part depend not only on the laser peening intensity, but also on the material and part geometry.

In addition, significant progress was made in defining the issues involved with modeling of residual stresses in thin sections, and determination of appropriate approaches to address these issues. Modeling of laser peening residual stresses in thin sections will not be possible until these issues are resolved.

Based on the modeling results, a follow-up task is needed to develop process optimization schemes to decrease the time and cost for process optimization. Funding sources are being sought for the follow-up effort.

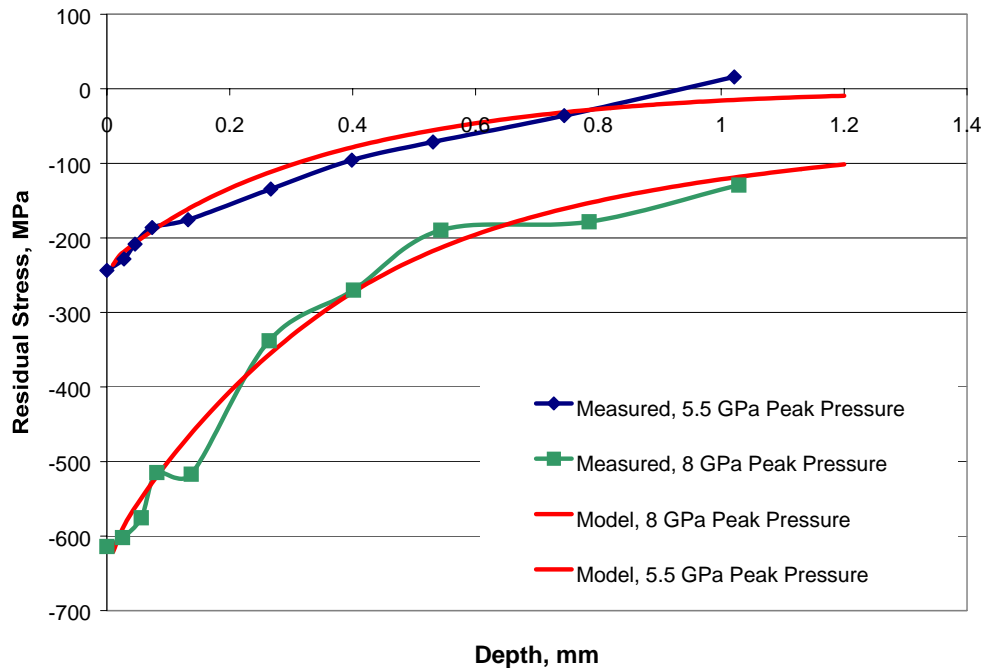


**FIGURE 6.** Comparison of Modeled and Experimental Residual Stresses for Similar Pressure Conditions

**Participating Organizations:** LSP Technologies, Inc., Ohio State University, University of Dayton Research Institute

**Points of Contact:**

Government

Mr. Joseph G. Burns  
U.S. Air Force  
AFRL/MLLN, Bldg. 655  
2230 Tenth St., Suite 1  
Wright-Patterson AFB, OH 45433-7817  
Phone: (937) 255-1360  
Fax: (937) 255-4840  
Email: Joseph.Burns@afrl.af.mil

Contractor

Dr. Allan H. Clauer  
LSP Technologies, Inc.  
6145 Scherers Place  
Dublin, OH 43016-1272  
Phone: (614) 718-3000 x12  
Fax: (614) 718-3007  
Email: allan.clauer-lspt@worldnet.att.net

## 1.5 RapidCoater™ for LSP

### *FY 97-00*

**Introduction:** One of the significant shortcomings of the current Laser Shock Peening process is slow processing, which is primarily due to the inability to remove the opaque overlay (paint) rapidly. Current practice requires the application and removal of the paint outside of the laser workstation. Under current practice, a part that requires multiple shots must be transported back and forth several times, from the laser workstation where it is peened, to a separate area where the overlay is removed, then back to the laser workstation, and so on. Sections 1.5.1 and 1.5.2 below explain what is being done to solve this problem. Section 1.5.1 describes the development, selection, and demonstration of a prototype system to rapidly remove the overlay system. Section 1.5.2 describes the development of a production system. The Points of Contact: and Participating Organizations listed below apply to both of these efforts.

**Participating Organizations:** LSP Technologies, Inc.

#### **Points of Contact:**

##### Government

Mr. David W. See  
U.S. Air Force  
AFRL/MLMP, Bldg. 653  
2977 P Street, Suite 6  
Wright-Patterson AFB, OH 45433-7739  
Phone: (937) 255-3612  
Fax: (937) 656-4420  
Email: David.See@afri.af.mil

##### Contractor

Dr. Allan H. Clauer  
LSP Technologies, Inc.  
6145 Scherers Place  
Dublin, OH 43016-1272  
Phone: (614) 718-3000 x12  
Fax: (614) 718-3007  
Email: allan.clauer-lspt@worldnet.att.net

## 1.5.1 Rapid Overlay Concept Development

### *FY 97*

**Background and Final Results:** The objectives of this program were to identify and evaluate promising methods for applying and removing the opaque overlay rapidly during laser peening. Two coating application methods were investigated: (i) water-soluble paint applied with a spray gun, and (ii) paint or ink application with an ink jet. The water-soluble paint/spray gun application method was selected as the most promising approach. The rapid overlay system concept was developed around this method. The rapid overlay demonstration test unit was assembled and tested to provide a working demonstration of the concept. The demonstration, which consisted of sequential application of the paint overlay, application of the overlay water film, firing the laser, and removal of the paint overlay in continuous, repetitive cycles, was successful. The successful demonstration system has been designated the RapidCoater™ System.

## 1.5.2 Development of a RapidCoater™ Manufacturing System

### *FY 98-00*

**Background:** The objective of this program is to develop a rapid-overlay-removal manufacturing system to be integrated into a production laser peening system. The production RapidCoater™ System should accommodate a range of parts and operate reliably at the laser repetition frequency. Another

objective is to develop a control system that will monitor the coating process and interface with the laser control system.

The ultimate objective of the Component Surface Treatment Action Team and of all the efforts described in this section is to develop an affordable Laser Shock Peening system. The relationship of all these efforts is shown below in Figure 7.

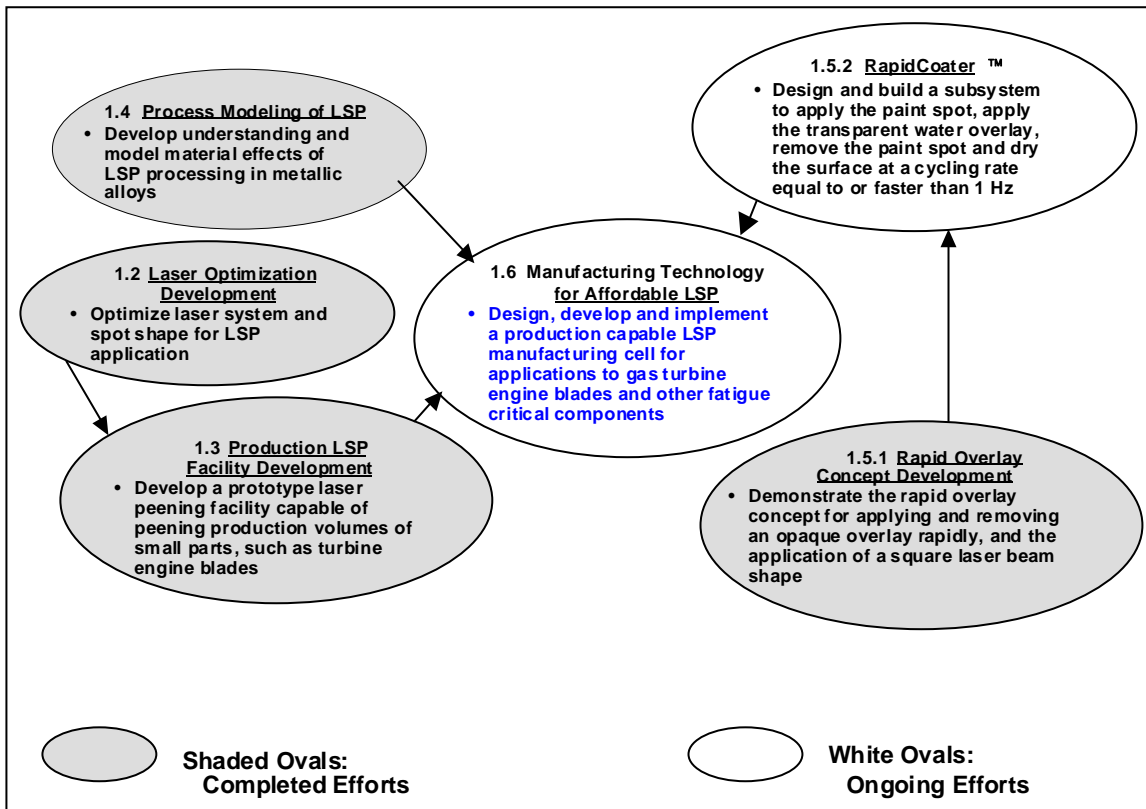


**FIGURE 7.** Interrelationship between LSP Programs

**Recent Progress:** A pre-prototype applicator head was successfully demonstrated. The resulting prototype applicator head has been built and will be demonstrated in 2000. A paint spot imaging technique was also demonstrated.

The RapidCoater™ will be demonstrated and spot-shaping techniques will be developed in a laser peening work cell, and the laser peening control system will be incorporated into the RapidCoater™.

## 1.6 Manufacturing Technology for Affordable LSP

*FY 98-02*

**Background:** The main activity of this program has been to prepare the facility for the various technical activities. The technical challenges associated with this program are all related to transitioning a prototype production facility into a full manufacturing facility. Additionally, the development and implementation of new (or improved) controls and monitors into the manufacturing facility will present individual technical challenges. This program has three phases.

Phase I: The purpose of Phase I is to mitigate the risks associated with the transition to manufacturing. This phase is divided into three areas:

1. Development and testing of new (or improved) controls and monitors, which will be used to increase the process reliability and reduce processing costs. The primary monitors (energy, temporal profile, and spatial profile) typically used for laser peening have been enhanced. “Secondary” laser monitors, process monitors, and quality control monitors are currently being demonstrated and will be down-selected for implementation into the new manufacturing cell.
2. Development of prototype small-parts and large-parts peening cells. This effort began in the final quarter of calendar year 1998 and is expected to be completed by the end of 1999.
3. Initial commercialization planning and new application development. Market surveys have been conducted and the commercialization plan is currently being drafted.

Phase II: Phase II is the final design and build phase for the laser and a small-parts peening cell. This phase is divided into two areas:

1. Design, fabrication, and integration of a manufacturing cell consisting of the laser system and a small-parts peening cell. This includes the down-selection and integration of the controls and monitors developed in Phase I.
2. Demonstration of the LSP manufacturing cell. The demonstration is currently scheduled for mid-year 2001.

Phase III: Phase III is the commercial development phase. The objective is to identify new applications in several market sectors, including the aerospace, medical, and automotive sectors. This is scheduled to begin in fiscal year 2000.

**Recent Progress:** Great progress has been made in completing the planned Phase I effort. The primary laser controls, which consist of the laser beam energy, temporal profile, and spatial profile, have been redesigned to be more robust. Additionally, new laser monitors have been developed to monitor the “health” of the laser. These new monitors include: monitoring the flashlamps to ensure that they are operating properly, monitoring energy reflected back from the part being processed (target backscatter), and monitoring critical optical components to ensure that they are not degrading.

A robust off-the-shelf distributed control network has been identified and successfully tested. This distributed control network will be incorporated into the design for the new laser system.

A prototype small-parts peening cell was completed. The peening cell, which was based upon the original peening cell already in place at LSPT, includes an improved beam delivery system, a more

robust beam monitoring configuration, and a more robust processing chamber. Lessons learned will be incorporated into the manufacturing cell.

Design of a large-parts peening cell was completed. Fabrication is in progress. The cell should be completed and available for use in early 2000.

Two market surveys were conducted: one by Pratt & Whitney of new applications within gas turbine engines, and one by an independent marketing firm that covered all other markets (excluding gas turbine engines). This information will be included in the commercialization plan that will be developed and delivered to the Air Force in December 1999.

Phase II work began ahead of schedule, which allowed for the following to occur ahead of plan:

- completion of the facility modifications,
- the start of the final manufacturing cell design, and
- acquisition of critical long-lead optical components.

The bulk of the remaining work is related to the assembly and fabrication of the laser and the associated peening cells. Implementation of the commercialization plan and the development of applications also remain to be done.

**Participating Organizations:** LSP Technologies, Inc.

**Points of Contact:**

Government

Mr. David W. See  
U.S. Air Force  
AFRL/MLMP, Bldg. 653  
2977 P Street, Suite 6  
Wright-Patterson AFB, OH 45433-7739  
Phone: (937) 255-3612  
Fax: (937) 656-4420  
Email: David.See@afrl.af.mil

Contractor

Dr. Jeff L. Dulaney  
LSP Technologies, Inc.  
6145 Scherers Place  
Dublin, OH 43016-1272  
Phone: (614) 718-3000 x11  
Fax: (614) 718-3007  
Email: jeff.dulaney-lspt@worldnet.att.net

## 1.7 Conclusion

The Component Surface Treatment Action Team demonstrated Laser Shock Peened (LSP'd) damaged turbine engine fan blades that had equal or better high cycle fatigue strength than undamaged unpeened blades; completed testing that showed the ability of the LSP process to stop both HCF crack initiation and propagation in these fan blades; demonstrated the complete LSP system (laser, facility; and more affordable process) with the prototype now available for government and industry use; and successfully transitioned the LSP technique to F101 and F110 engines. This has resulted in 15x increase in FOD tolerance for these engines, and major reduction in inspection man-hour costs, with increased flight safety. Due to the excellent progress to-date, all engine contractors are now pursuing LSP approaches. Further cost reduction of the manufacturing facilities and processes for the LSP technique is now the major focus of this team. Engine manufacturers are currently pursuing LSP on fan and compressor integrally bladed rotors (IBRs) and blisks.

## 2.0 MATERIALS DAMAGE TOLERANCE



### BACKGROUND

The Materials Damage Tolerance Research Action Team (Materials AT) is responsible for fostering collaboration between individual HCF materials damage tolerance research efforts, with the goal of reducing the uncertainty in the capability of damaged components by 50%. The Materials AT will provide technical coordination and communication between active participants involved in HCF life prediction, damage nucleation and propagation modeling, fracture mechanics methodology development, residual fatigue capability modeling, and the evaluation of surface treatment technologies. Annual technical workshops will be organized and summaries of these workshops will be disseminated to appropriate individuals and organizations. The Chair, Co-Chair, and selected Materials AT members will meet as required (estimated quarterly) to review technical activities, develop specific goals for materials damage tolerance research projects, and coordinate with the Technical Planning Team (TPT) and the Industry Advisory Panel (IAP). The Chairman (or Co-Chair) of the Materials AT will keep the TPT Secretary informed of AT activities on a frequent (at least monthly) basis. This AT will include members from government agencies, industry, and universities who are actively involved in materials damage tolerance technologies applicable to turbine engine HCF. The team is intended to be multidisciplinary with representatives from multiple organizations representing several component technologies as appropriate. The actual membership of the AT will change as individuals assume different roles in related programs.

### ACTION TEAM CHAIRS



#### Chair

Mr. Joseph G. Burns  
U.S. Air Force  
AFRL/MLLN, Bldg. 655  
2230 Tenth St., Suite 1  
Wright-Patterson AFB, OH 45433-7817  
Phone: (937) 255-1360  
Fax: (937) 656-4840  
Email: joseph.burns@afrl.af.mil



#### Co-Chair

Ms. Kathleen A. Sargent  
U.S. Air Force  
AFRL/PRTC  
1950 Fifth Street, Bldg. 18D  
Wright-Patterson AFB, OH 45433-7251  
Phone: (937) 255-2081  
Fax: (937) 255-2660  
Email: kathleen.sargent@wpafb.af.mil

### INTRODUCTION

Prior to this research program, no accurate techniques were available to determine the capability of materials subjected to variations in manufacturing, component handling, and usage. Such techniques are needed for accurate life prediction and optimized design to assure damage tolerance. The following pages summarize the schedules, backgrounds, and recent progress of the current and planned projects managed by this action team.

# Materials Damage Tolerance Research Schedule

Current & Planned Efforts	FY 95	FY 96	FY 97	FY 98	FY 99	FY 00	FY 01	FY 02
2.1 Microstructure Effects of Titanium HCF (Fan)								
2.2 Air Force In-House Research (Fan & Turbine)								
2.3 HCF & Time-Dependent Failure in Metallic Alloys for Propulsion Systems (Fan & Turbine)								
2.4 Improved HCF Life Prediction (Fan)								
2.5 Advanced HCF Life Assurance Methodologies (Fan & Turbine)								

## 2.1 Microstructure Effects of Titanium HCF (Fan)

*FY 96-98*

**Background:** The objective of this project was to determine the relationship between mean stresses and high cycle fatigue strength for Ti-6Al-4V by correlating the fatigue crack nucleation process with the cyclic deformation behavior of the alloy for different microstructures and crystallographic texture characteristics.

A workable hypothesis that was investigated was that high mean stress fatigue life sensitivity is associated with cyclic softening of Ti-6Al-4V, which in turn results in the absence of an endurance limit. In addition to establishing such a correlation, the second purpose of the investigation was to study the crystal orientation dependence on, and the microstructural features that affect, the cyclic deformation behavior. The specific factors that control crack nucleation are also being studied. The focus is on the formation of dislocation substructure and the statistical nature of crack formation. Analytical procedures emphasize the use of quantitative physical models that can be used to predict the mean stress sensitivity in this class of titanium alloys. The results should also be useful in the search for the best alloy/process for maximizing fatigue resistance in engineering structures.

**Final Results:** The findings of the two aspects of the physical behavior of Ti-6Al-4V that were investigated are described below. These findings contributed to the development of a model to predict the mean stress sensitivity of Ti-6Al-4V, which is also described below.

***Correlation of Cyclic Softening and the Absence of an Endurance Limit.*** Cyclic strain tests in strain control mode did not reveal significant differences in cyclic deformation behavior between the investigated microstructures (lamellar cross-rolled, bimodal fine uni-rolled, bimodal coarse cross-rolled, bimodal coarse forged, equiaxed coarse cross-rolled, and equiaxed coarse forged). All six microstructures underwent cyclic softening, and the saturation stresses at all strain levels (and hence, cyclic stress-strain curves) were almost identical for all of these microstructures. However, in the initial condition (monotonic stress-strain curve), the differences in saturation stresses were much greater. Unlike S-N (stress-life) curves, little difference was observed between the  $\epsilon$ -N (strain-life) curves generated for each of the investigated microstructures, especially at low strains. Also, relatively little scatter was observed for each curve.

***Effect of Crystal Orientation and Microstructural Features on Fatigue Behavior.*** Of the six microstructure/texture combinations investigated, bimodal fine uni-rolled and lamellar cross-rolled displayed superior fatigue properties to the remaining four microstructures (bimodal coarse cross-rolled, bimodal coarse forged, equiaxed coarse cross-rolled, and equiaxed coarse forged). Bimodal fine uni-rolled and lamellar cross-rolled microstructures exhibited Goodman dependence of fatigue strength, while the other four microstructures had anomalous mean stress dependence, with fatigue strength values at intermediate mean stresses being considerably lower than predicted by the Goodman relation.

***Analytical Procedures (Models) to Predict Mean Stress Sensitivity.*** The fatigue data collected in this project have been statistically analyzed to develop a model to predict the effects of microstructure and texture on the fatigue strength of  $\alpha/\beta$  titanium alloys. This effort resulted in a model that allows the accurate prediction of fatigue curves for titanium alloys from microstructure and texture characteristics at different R ratios ( $\sigma_{\min}/\sigma_{\max}$ ). Separate models have been developed for low cycle and high cycle fatigue regimes, and for three ranges of R:  $R < 0$  (tensile-compressive loading),  $0 \leq R \leq 0.5$  (tensile-tensile loading) and  $0.5 < R \leq 0.7$  (creep-fatigue interaction). For each of these regimes, fatigue strength

is calculated as a function of alpha grain size  $d_\alpha$ , transformed beta volume fraction  $v_\beta$ , texture orientation parallel to test direction  $X_\alpha$ , ultimate tensile strength  $U$ , and ductility (reduction of area)  $e_f$ . Figure 8 demonstrates how the model (presented with solid curves) fits actual data points for three different microstructures at  $R=0.1$ . The following equations were used to construct these curves:

1. LCF regime,  $0 \leq R \leq 0.5$

$$\sigma_L = 101.457 + 5.565 v_\beta + 21.562 \sqrt{d_\alpha} - 44.629 e_f - 1.077 X_\alpha - 6.227 \sqrt{d_\alpha} \log N - 0.21 U R$$

2. HCF regime,  $0 \leq R \leq 0.5$

$$\sigma_H = 91.859 + 10.427 v_\beta - 8.529 \sqrt{d_\alpha} - 5.208 \log N - (10.684 / \sqrt{d_\alpha} + 0.164 U) R$$

where:  $d_\alpha$  = alpha grain size,  $\mu\text{m}$   
 $v_\beta$  = transformed beta volume fraction  
 $X_\alpha$  = texture orientation parallel to test direction (x random)  
 $U$  = ultimate tensile strength (Ksi)  
 $e_f$  = ductility (reduction of area)  
 $N$  = number of cycles  
 $R$  = stress ratio ( $\sigma_{\min}/\sigma_{\max}$ )

The model was tested on the investigated microstructures, and accurately predicted the fatigue strength of  $\alpha/\beta$  titanium alloys for the following range of parameters:

$d_\alpha = 3\text{-}16 \mu\text{m}$   
 $v_\beta = 0.15\text{-}0.80$   
 $X_\alpha = 4\text{-}13$   
 $U = 138\text{-}173 \text{ Ksi}$   
 $e_f = 0.30\text{-}0.55$

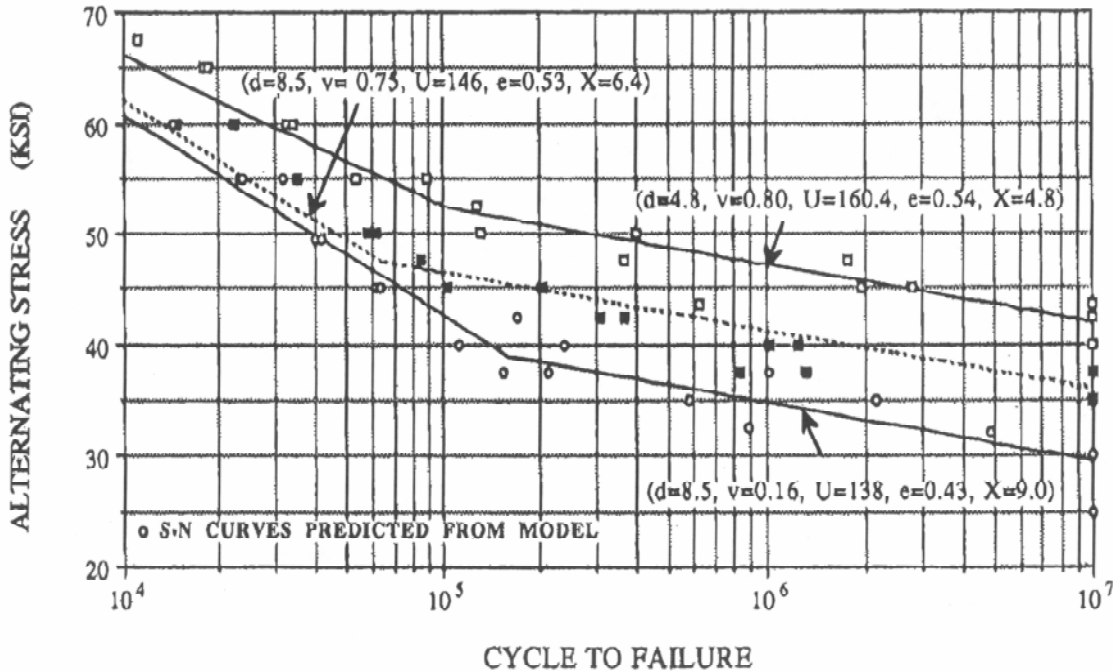


**FIGURE 8.** S-N Input Data and Fatigue Strength Model Results for Bimodal Fine Uni-Rolled, Bimodal Forged, and Equiaxed Forged Microstructures (Top to Bottom) at  $R=0.1$

**Participating Organizations:** Air Force Office of Scientific Research (AFOSR), Worcester Polytechnic Institute, Pratt & Whitney

**Points of Contact:**

Government

Dr. Spencer Wu  
U.S. Air Force, AFOSR/NA  
110 Duncan Ave., Suite B115  
Bolling AFB, DC 20332-8080  
Phone: (202) 767-4989  
Fax: (202) 767-4988  
Email: spencer.wu@afosr.af.mil

Contractor

Prof. Richard D. Sisson, Jr.  
Worcester Polytechnic Institute  
Mechanical Engineering Department  
100 Institute Road  
Worcester, MA 01609  
Phone: (508) 831-5335  
Fax: (508) 831-5178  
Email: sisson@wpi.edu

## 2.2 Air Force In-House Research (Fan & Turbine)

*FY 96-03*

**Background:** The objectives of this program are as follows:

- (1) Conduct breakout research on titanium and nickel-base superalloys.
- (2) Explore high cycle fatigue related damage mechanisms, including the determination of the relative significance of specific damage mechanisms and the identification of specific areas requiring a concentrated research and development effort for incorporation into the HCF design system.
- (3) Develop innovative test techniques and modeling concepts to guide the industry research program.
- (4) Conduct research and evaluation to demonstrate and validate damage tolerance design methodologies for HCF.

**Recent Progress:** During the past year, progress has been made in all areas. The following paragraphs highlight specific accomplishments with regard to the approaches being taken in this task.

❖ **Material Behavior for Modeling.** Testing has been accomplished to generate valid data for modeling the damage mechanisms associated with high cycle fatigue interaction with low cycle fatigue (LCF), fretting fatigue, and foreign object damage (FOD).

- *High Cycle Fatigue / Low Cycle Fatigue Interaction.* A study is currently being performed to determine the influence of load history on the initiation of cracks under LCF loading and its subsequent influence on HCF thresholds for both small and large cracks. This study is being performed on notched fatigue specimens with crack initiation being detected with DC potential difference. In this study, cracks are initiated in LCF loading at  $R = -1$  and  $0.1$ , and the HCF thresholds for high cycle fatigue stress ratios of  $R=0.1$  and  $0.5$  are determined from fracture stresses and crack sizes. Heat tinting is used to verify crack size and shape. The step test method is used to apply the HCF loading as described in Figure 9. The HCF load level is ramped up by 5% after  $10^7$  cycles if no crack growth is detected within the load block. This process is repeated until fracture occurs.

The HCF crack thresholds determined in the above manner varied with load sequence. However, when specimens were stress relief annealed after LCF pre-cracking (prior to HCF loading), the HCF thresholds were consistent for a given HCF stress ratio as shown in Figure

10. Moreover, the HCF thresholds for small cracks were consistent with the large crack threshold for a given stress ratio. This indicates that the LCF / HCF threshold appears to be dependent on load history. Consistent results also indicate that when LCF cracks are present, there exists an HCF threshold level below which cracks don't grow. Also, preliminary results indicate there is no "small crack" effect down to  $c = 60\mu\text{m}$ .

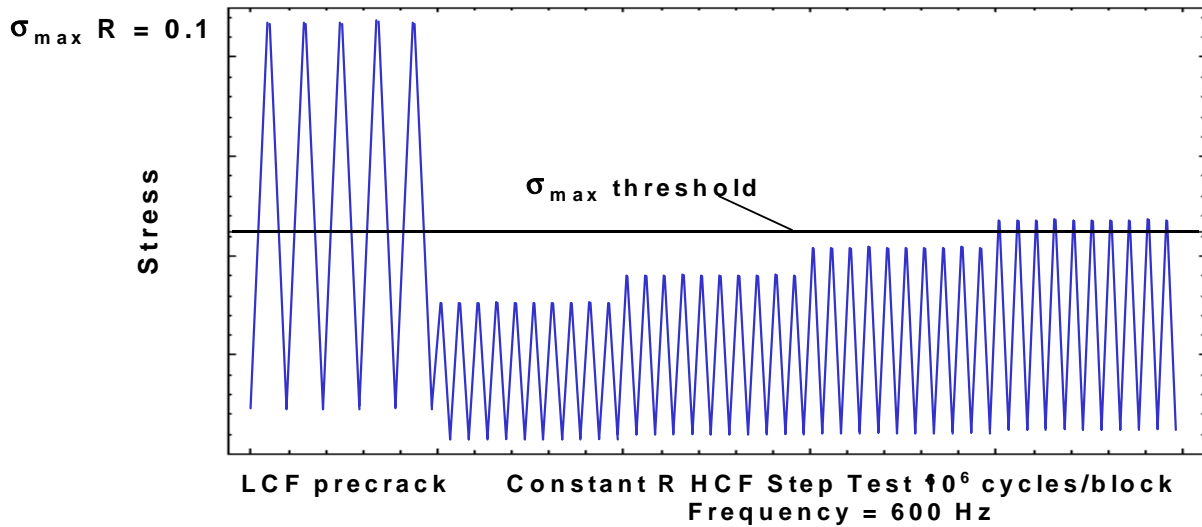


**FIGURE 9.** Pre-Crack and Step-Test Loading Technique Used to Determine LCF/HCF Thresholds

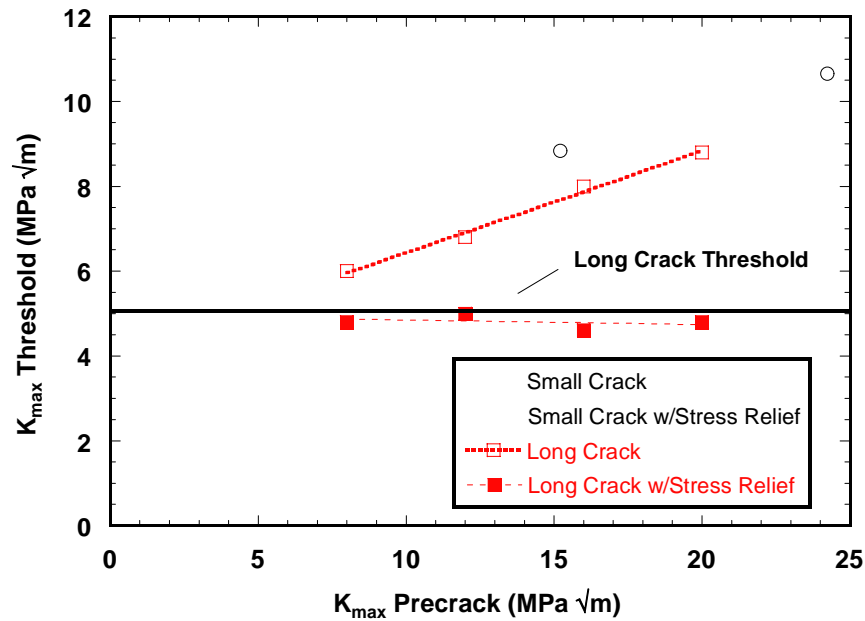


**FIGURE 10.** LCF/HCF Thresholds for HCF Stress Ratio  $R=0.1$

- *HCF Fretting Fatigue.* Four studies and a modeling effort on fretting fatigue are being accomplished in this program:
- The identification of fretting fatigue failure mechanisms and the effect of fretting fatigue damage on residual HCF strength was investigated. The geometry in the test apparatus employed flat fretting pads on either side of a flat uniaxial fatigue specimen with the fretting pads having a radius at the edge of contact. The test configuration, which employs identical gripping at both ends of the specimen, via the fretting pads, produced two nominally identical fretting fatigue tests per specimen. Fretting damage occurred at both ends of the specimen at the edges of contact. All tests were conducted at constant frequency of either 300 or 400 Hz in lab air at room temperature. A range of shear forces (proportional to the axial stress in the specimen), and the resultant shear stress distribution was achieved by varying the contact length and the contact radius using a range of pad geometries, and by varying the normal contact load.
- Test results indicate that for a given condition of contact radius and applied stress ratio, the axial stress in the specimen corresponding to a fatigue life of  $10^7$  cycles is relatively independent of normal stress. Therefore, for the current study, two normal stresses (140 MPa and 420 MPa) were selected. These stresses represent values that are typical of the upper and lower limit of normal stresses observed in some fan-blade dovetail attachments. A contact radius of 3.2 mm, and a fretting fatigue stress ratio of  $R=0.5$  were chosen because of the similarity to dovetail geometry and loading conditions. Three levels of damage were investigated:  $10^4$ ,  $10^5$ , and  $10^6$  cycles, which correspond to 0.1, 1.0, and 10 percent of the  $10^7$  cycle life, respectively. Samples tested under uniaxial conditions at  $R = 0.1$  with a normal load of 140Mpa did not result in measurable reduction in residual axial fatigue strength due to fretting fatigue. Additional testing is underway.
- Elastic-plastic finite element analyses (FEA) of a cylinder-on-plate configuration studied in the laboratory were performed to provide an explanation for the decrease in fretting fatigue life with increasing contact pressure. Three values of normal load, namely 1338 N, 2230 N and 3567 N, and three stress ratios (0.1, 0.5 and 0.7) were considered. Based on a previously determined dependency between contact pressure and friction coefficient, the effect of the coefficient of friction was also evaluated. The deformation remained elastic under all the conditions examined. Cyclic, interfacial stresses and slips were analyzed in detail. The amplification of the remotely applied cyclic stress in the contact region was shown to provide a rationale for the effect of contact pressure and stress amplitude on life. Comparisons with previous experiments indicate that the local stress range computed using finite element analysis may be sufficient for predicting fretting fatigue life. Further, results suggest that the slip amplitude and shear tractions may be neglected for this purpose.
  - An investigation of fretting fatigue crack initiation behavior in Ti-6Al-4V was performed. Fretting fatigue contact parameters were varied through the modification of the fretting pad geometry which included two different radii of cylindrical contact (50.8mm and 101.6mm) and flat contact with edge radii. The applied tensile loads were also varied to obtain fretting fatigue crack initiation in both the low and high cycle fatigue regimes. The salient features of the fretting fatigue experiments were modeled and analyzed with finite element analysis. The results of the finite element analyses were used to formulate and evaluate several fatigue parameters. The fretting fatigue specimens were examined to determine the crack location and the crack orientation along the contact surface. The fatigue parameters were evaluated on their ability to predict these observations and they were used to compare fretting fatigue with uniaxial (no fretting) fatigue data. The comparison of the analysis and

experimental results showed that fretting fatigue crack initiation is dependent on the plane of maximum shear stress amplitude and the slip range at this location.

➤ *HCF and Foreign Object Damage.* Three studies are being performed in this area:

- The effects of notch sizes on HCF capability ( $10^6$  cycles) have been investigated. Three different notch sizes, each with a stress concentration factor of  $K_t = 2.78$ , were tested to determine whether or not  $K_t$  was a valid parameter for assessing FODed and/or notched material capability. Results demonstrated a definite notch size effect in Ti-6Al-4V that can be influenced by the material product form and microstructure. Also, no single parameter is adequate for characterizing the notch size effect. Important considerations include material condition, notch root radius, local stress field, and notch root plasticity.
- An investigation was performed in which four different methods of simulating FOD (impact by glass spheres and steel spheres, and quasi-static indenting and notch shearing by steel chisels with controlled tip radii) were evaluated to determine their effects on Ti-6Al-4V fan-blade specimen fatigue capability. Finite element methods were also utilized to model the impact events and to build an understanding of the effect of the residual stress state on the capability of damaged specimens and to determine a criterion to predict HCF failure after damage by simulated FOD.

Results indicate that by calculating the real stress state in Ti-6Al-4V that has been damaged by simulated FOD, the conditions under which it will fail from high cycle fatigue can be predicted. This failure will occur when the stress state in the vicinity of the damage is as severe as the fatigue strength of undamaged Ti-6Al-4V.

The total depth into a specimen from its edge to the maximum extent of the plastically deformed zone ( $D_d$ ) was found to be a damage quantification parameter that yielded a simple empirical relationship with the reduction in fatigue strength. It is clearly the size of the notch plus the size of the plastic damage zone that reduces the fatigue strength of Ti-6Al-4V. But when the parameter  $D_d$  is used, damage created by all techniques investigated in this study produced identical reductions in fatigue strength, within the statistical variation.

The smallest amounts of total damage that could be generated were about 500  $\mu\text{m}$  (92  $\mu\text{m}$  notch depth with 400  $\mu\text{m}$  plastic zone). At these levels of damage, the fatigue strength is nearly the same as that of undamaged Ti-6Al-4V. At greater damage depths, all damage mechanisms evaluated in this study show a linear decrease in fatigue strength with increasing damage depth until it reaches 1750  $\mu\text{m}$ . At damage depths larger than 1750  $\mu\text{m}$ , a stress threshold appeared below which no specimen failures occurred. This may be because these notches approach the ‘worst case notch’ conditions; i.e., notches with initial cracks that will not propagate at stresses below the threshold level.

It was also found that impacts by glass spheres between 2 mm and 5 mm in diameter and 2 mm diameter steel spheres at realistic FOD velocities can be adequately simulated more economically by indentation techniques that use chisels of various radii to create damage so long as the total damage depth is matched (not just the visible crater dimensions).

- A detailed systematic evaluation of macroscopic and microscopic damage generated by all FOD impact conditions is being performed for the laboratory FODed specimens. Currently, the damage created by the impact by 1-mm-diameter glass spheres (300 m/sec) on the leading edge of simulated fan-blade test specimens is being characterized. Impact from steel spheres and quasi-static indents will be performed in the future.

❖ **Investigation of Other Damage Mechanisms.** Two studies are being performed in this area.

- The characterization of the effect of laser shock peening (LSP) is important for understanding the increase in fatigue strength and foreign object damage (FOD) tolerance for turbine engine components. These enhanced fatigue properties are a direct result of compressive residual stresses found in the treated regions. This study will seek to explore the effects of power density and pulse repetition on the residual stresses, fatigue crack growth properties, and microstructure / substructure development of a Ti-6Al-4V simulated airfoil.

Little microstructural deformation was found in SEM examinations. TEM studies showed a large increase in dislocation density after laser shock peening. It was found that the residual stress state and percent cold work were a function of both the LSP power density and the number of laser pulses per spot. In addition, there was a strong correlation between the magnitude of residual compressive stresses generated and the percent cold work measured. Fatigue cracks in LSPed blades would frequently arrest until increased loads were applied.

Figure 11 depicts a typical in-depth residual stress profile generated by two sets of LSP parameters. The residual stresses were measured through half the nominal airfoil thickness. It is clear that the higher intensity treatment (9 GW/cm<sup>2</sup> as opposed to 4 GW/cm<sup>2</sup>) produced a more intense state of compressive residual stress throughout the thickness.

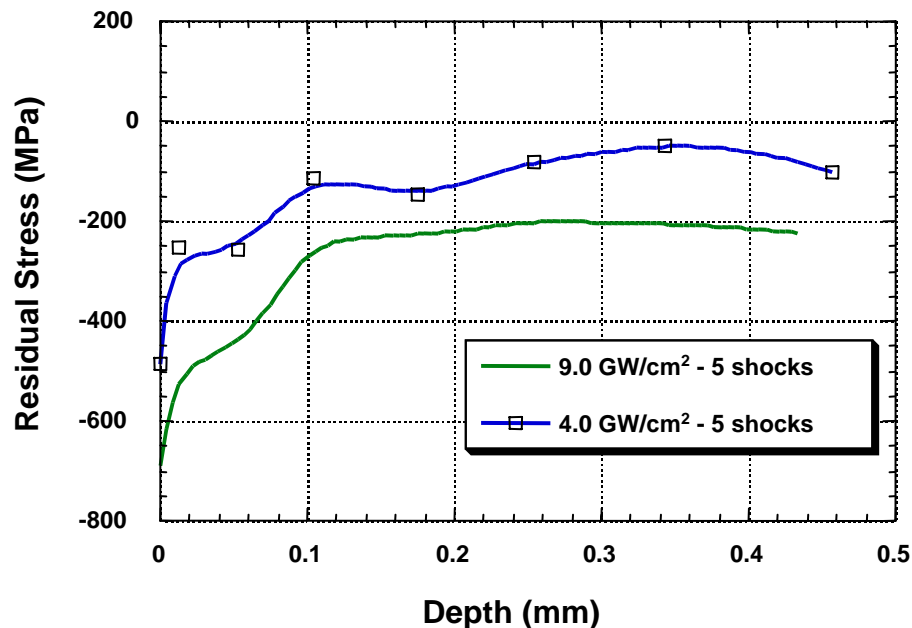


**FIGURE 11.** Residual Stress vs. Depth for Five Shocks per Spot

- A study on the effects of pre-straining on material HCF capability was conducted to evaluate the effect of material pre-straining at FOD impact sites. Bulk material (Ti-6Al-4V) was upset forged

to a strain level of 10% at room temperature. Specimens were then machined from the pre-strained material and both “as received” and pre-strained specimens were tested at 400 Hz under pure HCF loading using the step-test method to determine material maximum stress capability (fatigue limit stress) at  $10^7$  cycles. As shown in Figure 12, pre-strained specimens show a possible slight decrease in fatigue limit stress at  $R=0.1$  and  $0.5$ . Additional testing of pre-strained specimens at a pre-strain level of 15% will be pursued in the next year.

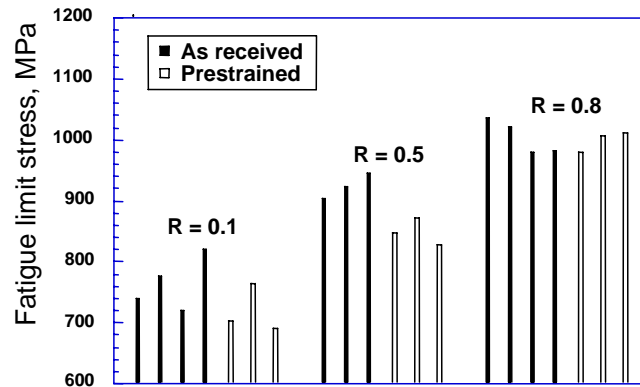


**FIGURE 12.** Comparison of Pre-Strained and “As Received” Material Fatigue Limit Stress at  $10^7$  Cycles

- ❖ ***Innovative Test Technique Development.*** A new fretting fatigue test apparatus has been developed that imparts both LCF and HCF stresses similar to those experienced by fan blades in the dovetail region of the blades. At the contact region, steady-state and temporal normal stresses, shear stresses, torsional stresses, and a moment are imparted on the blade / hub interface. These loads are a result of the centrifugal loads due to engine rotation (low cycle fatigue loading – steady-state), and the (temporal) vibrational loads imparted by aerodynamic loading. The experimental set-up shown in Figure 13 enables both static loading and a dynamic axial load to be applied in the dovetail region.



**FIGURE 13. New HCF/LCF Fretting Fatigue Test Apparatus**

**Participating Organizations:** Air Force Research Laboratory (AFRL); University of Dayton Research Institute; Systran Corporation; Southern Ohio Council on Higher Education; University of Portsmouth, United Kingdom; Air Force Institute of Technology

**Points of Contact:**

**Government**

Dr. Theodore Nicholas  
U.S. Air Force  
AFRL/MLLN, Bldg. 655  
2230 Tenth St., Suite 1  
Wright-Patterson AFB, OH 45433-7817  
Phone: (937) 255-1347  
Fax: (937) 656-4840  
Email: theodore.nicholas@afrl.af.mil

**Government**

Mr. Joseph G. Burns  
U.S. Air Force  
AFRL/MLLN, Bldg. 655  
2230 Tenth St., Suite 1  
Wright-Patterson AFB, OH 45433-7817  
Phone: (937) 255-1360  
Fax: (937) 656-4840  
Email: joseph.burns@afrl.af.mil

## **2.3 HCF & Time-Dependent Failure in Metallic Alloys for Propulsion Systems (Fan & Turbine)**

***FY 96-01***

**Background:** This program is focused on the definition, microstructural characterization, and mechanism-based modeling of the limiting states of damage associated with the onset of high cycle fatigue failure in titanium and nickel-base alloys for propulsion systems. The goal of this program is to provide quantitative physical/mechanism based criteria for the evolution of critical states of HCF damage, enabling life prediction schemes to be formulated for fatigue-critical components of the turbine engine. The specific objectives are as follows:

- (1) Perform systematic experimental studies to define crack formation and lower-bound fatigue thresholds for the growth of “small” and “large” cracks at high load ratios, high frequencies, and with superimposed low cycle fatigue loading, in the presence of primary tensile and mixed-mode

loading; and analyze the applicability of the threshold stress-intensity factors to characterize crack initiation and growth in engine components subjected to high cycle fatigue.

- (2) Define lower-bound fatigue thresholds for crack formation in the presence of notches, fretting, or projectile damage, on surfaces with and without surface treatment (e.g., shot or laser shock peened).
- (3) Develop an understanding of the nature of projectile (foreign object) damage and its mechanistic and mechanical effect on initiating fatigue crack growth under high cycle fatigue conditions.
- (4) Develop new three-dimensional computational and analytical modeling tools and detailed parametric analyses to identify the key variables responsible for fretting fatigue damage and failure in engine components; compare model predictions with systematic experiments; and identify and optimize microstructural parameters and geometrical factors and surface modification conditions to promote enhanced resistance to fretting fatigue.
- (5) Develop mechanistic models of the initiation and early growth of small cracks to characterize their role in HCF failure, with specific emphasis on initiation at microstructural damage sites and on subsequent interaction of the crack with characteristic microstructural barriers; and correlate such models to experimental measurement.

**Recent Progress:** Considerable progress has been made during the third year of this research program. Specific accomplishments are outlined below:

❖ *HCF/LCF Interactions.*

- Worst-case fatigue threshold stress intensities have been measured in STOA (Solution Treated and Over Aged,  $\alpha+\beta$ -processed) Ti-6Al-4V using large ( $> 5$  mm) cracks under representative HCF conditions ( $R > 0.95$ , 1,000 Hz). A number of different methods were investigated to determine the fatigue threshold stress intensity factors. With constant- $K_{\max}$  cycling at 1 kHz, a “worst-case” threshold can be defined in Ti-6Al-4V at  $\Delta K_{th} = 1.9 \text{ MPa } \sqrt{\text{m}}$  (Fig. 14). To verify this “worst case” approach, the high-load-ratio fatigue crack propagation data are compared to fatigue data from small cracks, which includes both naturally-initiated small cracks ( $\sim 45\text{--}1,000$   $\mu\text{m}$ ) and to small cracks ( $< 500$   $\mu\text{m}$ ) emanating from sites of foreign object damage. In both cases, crack growth is not observed below  $\Delta K \sim 2.9 \text{ MPa } \sqrt{\text{m}}$ , (Fig. 15). Consequently, it is believed that the “worst-case” threshold concept can be used as a practical lower bound for the stress intensity required for the onset of small-crack growth under HCF conditions.

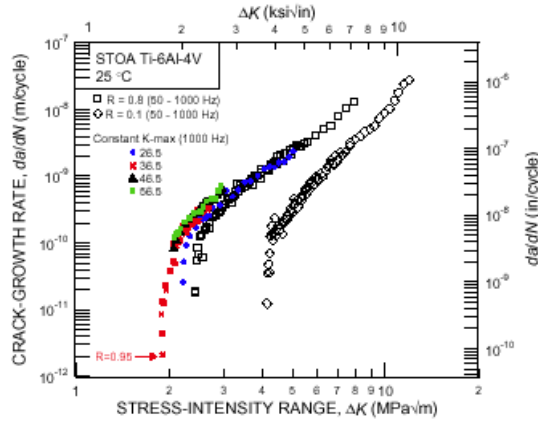


**FIGURE 14.** Constant- $K_{\max}$  fatigue crack propagation behavior at four different  $K_{\max}$  values:  $K_{\max} = 26.5, 36.5, 46.5$ , and  $56.5$   $\text{MPa} \sqrt{\text{m}}$  (1,000 Hz) compared to constant- $R$  data at  $R = 0.1$  and  $0.8$  (50-1,000 Hz).

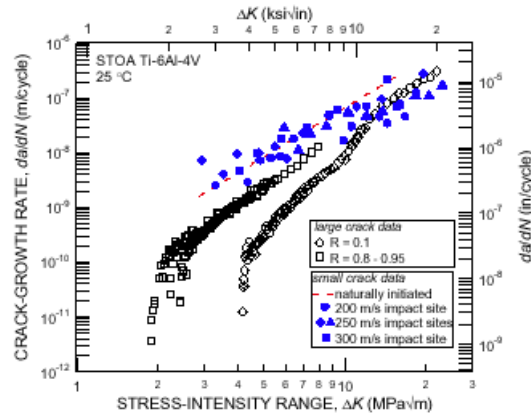


**FIGURE 15.** Comparison of long-crack propagation data to fatigue data from small cracks (including both naturally-initiated small cracks and those originating from sites of foreign object damage).

- Large-crack threshold behavior in a polycrystalline nickel-base disk alloy has been characterized at 1,000 Hz at 22° and 650-900°C, with respect to the role of microstructure, frequency and load ratio. Two different microstructures of KM4 are being studied. By varying the heat treatment, the grain size is varied from around 6 microns (sub-solvus heat treatment) to 55 microns (super-solvus heat treatment). Room temperature results indicate that coarse-grained material had better fatigue crack propagation resistance and higher thresholds than fine-grained material. Also, higher load ratios led to lower fatigue crack propagation resistance at equivalent  $\Delta K$ . At 650°C, thresholds at 1,000 Hz are approximately 15-20% higher than those at 100 Hz for both microstructures. Also, thresholds in the fine-grained material are approximately 5-10% higher than in the coarse-grained material at both frequencies.

#### ❖ *Notches and Foreign Object Damage (FOD).*

- FOD was simulated by high-velocity (200-300 m/s) impacts of 3.2 mm diameter steel spheres on a flat surface at 90° impact angle. At velocities above 250 m/s, pronounced pile-ups at the crater rim with some detached material were formed as is shown for 300 m/s impact in the scanning electron micrograph (Fig. 16). Of critical importance were the observations, shown in Figs. 17, that for the highest velocity impacts at 300 m/s, plastic flow of material at the crater rim causes local notches (Fig. 17a) and even microcracking (Fig. 17b). The microcracks were quite small, i.e., between ~2 to 10  $\mu\text{m}$  in depth, but clearly provided the nucleation sites for subsequent HCF cracking, as shown in Figure 17c. No such microcracking could be detected in this alloy at lower impact velocities.

To date, no crack growth from FOD impact (or naturally-initiated) sites has been observed at  $\Delta K$  values below  $\sim 2.9 \text{ MPa} \sqrt{\text{m}}$ . This is over 50% higher than the “closure-free”, *worse-case* threshold value of  $\Delta K_{\text{th}} = 1.9 \text{ MPa} \sqrt{\text{m}}$ , defined for large cracks in bimodal Ti-6Al-4V at the highest possible load ratio ( $R \sim 0.95$ ). Consequently, it is concluded that fatigue-crack

propagation thresholds for large cracks, determined under conditions that minimize crack closure, can be used as lower bounds for the threshold stress intensities for naturally-initiated and FOD-initiated small cracks in this alloy.

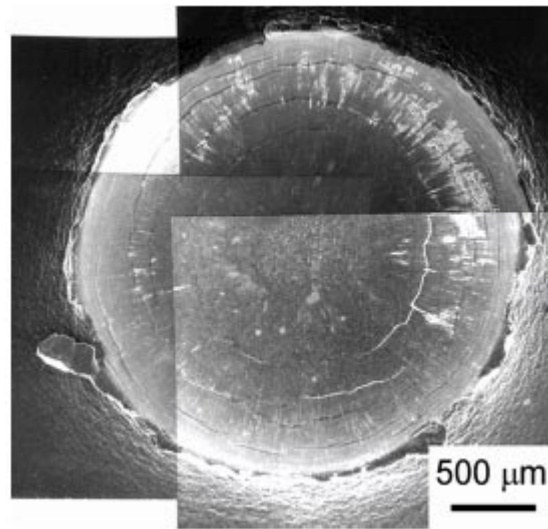


**FIGURE 16.** Scanning electron micrographs of impact damage sites for a 300 m/s impact velocity, indicating lip formation at crater rim and intense shear band formation emanating at the indent surface.

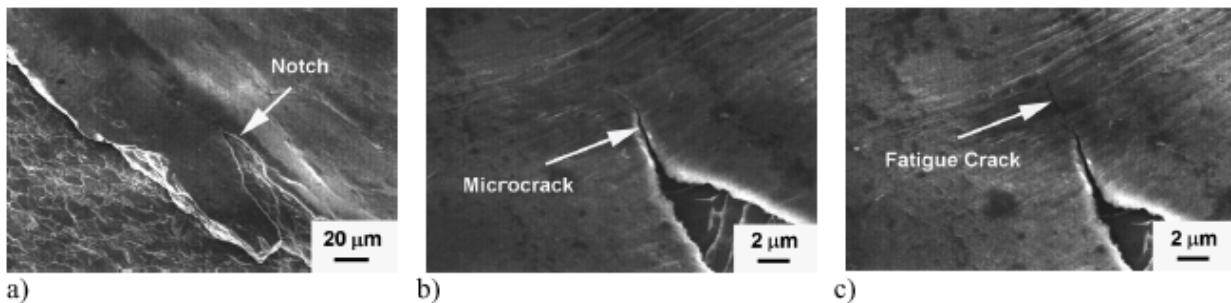


**FIGURE 17.** Scanning electron micrographs showing the presence of microcracking at crater rim of a FOD indent after the highest velocity (300 m/s) impacts. Micrographs show (a) local notches at crater rim caused by plastic flow of material, (b) microcracks emanating from such notches, and (c) subsequent fatigue-crack growth initiated at such microcracks after 5,000 cycles at  $\sigma_{\max} = 500$  MPa ( $R = 0.1$ ).

- Efforts are currently underway to utilize a 300  $\mu\text{m}$  spot size at the Stanford Synchrotron Radiation Laboratory and a 1  $\mu\text{m}$  spot size at the Advanced Light Source at the Lawrence Berkeley National Laboratory to characterize the stress fields surrounding a damage site caused by a hard-body impact. Based on preliminary results, it is evident that synchrotron x-ray diffraction is a useful tool for characterizing the strain distribution associated with foreign object damage; however, further technique refinement is necessary to more completely characterize the damage state.

## ❖ *Fretting Fatigue.*

- Mixed-mode crack-growth thresholds were measured in  $\alpha+\beta$  processed Ti-6Al-4V using the asymmetric four-point bend geometry at mixities of  $K_{II}/K_I \sim 0$  to 7.1. Mixed-mode loading conditions were quantified, both in terms of the ratio of  $\Delta K_{II}$  to  $\Delta K_I$  and the phase angle,  $\beta$  ( $= \tan^{-1} (\Delta K_{II} / \Delta K_I)$ ). Results indicate that when fatigue-crack growth in this alloy is characterized in terms of the crack-driving force  $\Delta G$  (range in strain energy release rate), which incorporates both the applied tensile and shear loading, the mode I fatigue-crack growth threshold is a lower bound (worst case) with respect to mixed-mode (I + II) crack-growth behavior. This result indicates that, for cracks of sufficient length, the presence of mixed-mode loading does not preclude the application of a threshold-based design methodology.
- Stress-intensity solutions have been developed for small, semi-elliptical, surface cracks under mixed-mode loading. Such solutions are being used to experimentally measure (for the first time) small-crack, mixed-mode thresholds in Ti-6Al-4V.
- A continuum level mechanics model (Adhesion Model) that incorporates interfacial adhesion, material properties and contact loads has been developed for predicting contact fatigue crack initiation for a variety of loading states and contact geometries. This model enables the analysis of a variety of contact problems from those due to fretting fatigue in large-scale structures to contact fatigue in micro-scale devices.
- The influence of contact and bulk stresses, contact geometry, material microstructure, and surface finish on the fretting fatigue behavior of Ti-6Al-4V has been investigated through controlled experiments using the MURI-developed fretting fatigue device. The observed fretting damage scars (contact area and the stick-slip zone) correlated well with theoretical predictions. Qualitatively, four different stages (crack initiation, small-crack propagation, long-crack propagation and catastrophic failure) in the fretting fatigue life of a test component were identified. Quantitatively, conditions for crack initiation were analyzed within the context of the adhesion model and a modified Crossland analysis was conducted. By accounting for the steady-state long crack growth life through a Paris law formulation, crack initiation and small crack propagation lives were also identified.
- Work has begun on quantitative analytical and experimental tools for evaluating the effectiveness of different palliatives (e.g., shot peening, laser shock peening, and coatings) for fretting fatigue.

**Participating Organizations:** Air Force Office of Scientific Research (AFOSR), University of California at Berkeley, Massachusetts Institute of Technology, Michigan Technological University, Harvard University, Southwest Research Institute, Imperial College, London University, Technische Universität Hamburg-Harburg, Universität für Bodenkultur (BOKU)

### **Points of Contact:**

#### Government

Major Brian Sanders, Ph.D.  
U.S. Air Force, AFOSR/NA  
110 Duncan Avenue, Suite B115  
Bolling AFB, DC 20332-0001  
Phone: (202) 767-6063  
Fax: (202) 767-4988  
Email: brian.sanders@afosr.af.mil

#### Contractor

Prof. Robert O. Ritchie, Ph.D., Sc.D.  
University of California at Berkeley  
Dept. of Materials Science and Mineral Engineering  
Berkeley, CA 94720-1760  
Phone: (510) 486-5798  
Fax: (510) 486-4995  
Email: roritchie@lbl.gov

## 2.4 Improved HCF Life Prediction (Fan)

*FY 96-00*

**Background:** The focus of this program is on the development of damage tolerant design processes for gas turbine engines that substantially reduce the potential occurrence of high cycle fatigue failures in titanium (fan) structures. Specific objectives for this program are: (1) to characterize in-service damage associated with high-cycle fatigue loading of titanium fan blades; (2) to develop techniques to generate damage states in the laboratory that are representative of in-service damage; (3) to model the nucleation and progression of damage in titanium fan blades; and (4) to develop an improved damage tolerant life prediction and design methodology for turbine engine rotating structures subjected to high cycle fatigue (HCF) and combined high and low cycle fatigue (HCF/LCF) loadings.

This program is being accomplished through the development of a better understanding of the three primary damage mechanisms experienced in the fan section, and the transitioning of that understanding into the development of improved damage tolerance life prediction methodologies. All experimental studies are being performed on an  $\alpha+\beta$  processed Ti-6Al-4V forged plate, specifically produced to provide a representative titanium alloy with consistent properties that would minimize data scatter due to material inhomogeneities. Specifically, this program is being performed through the accomplishment of research in the following areas:

- ❖ *HCF/LCF Interactions* research is aimed at developing a better understanding of the fatigue and crack growth damage accumulation processes due to the load interactions generated in LCF/HCF loading. This includes the study of fatigue crack threshold behavior for both pristine and LCF damaged material (with various surface treatments), as well as the development of baseline material data for comparison with other damage modes.
- ❖ *Foreign Object Damage* research is aimed at developing a better understanding of the occurrence and levels of FOD in different sections of turbine engines and characterizing the relevant parameters for modeling FOD damage progression. Techniques for reproducing damage representative of in-service FOD are being investigated, and specimens containing laboratory-induced FOD will be tested to characterize the effects of FOD.
- ❖ *Fretting Fatigue* research is aimed at developing a better understanding of the occurrence and levels of fretting fatigue damage at the fan blade root / disk hub interface. Techniques for reproducing damage representative of in-service fretting fatigue are being investigated and specimens containing laboratory-induced fretting and fretting fatigue damage will be tested to characterize the effects of fretting fatigue on the HCF behavior. Criteria for the initiation and propagation of cracks under fatigue in contact regions will be developed.
- ❖ *Damage Tolerant Life Prediction Methodologies* research is aimed at utilizing data generated to characterize the damage mechanisms described above to develop new, more accurate methods of modeling the initiation and progression of damage in titanium fan blades. Existing methodologies will be modified where possible, and new methodologies will be developed as necessary. Validation of life prediction methodologies will be accomplished through the comparison of predictions to experimental and service data.

**Recent Progress:** During the past year, progress has been made in the following areas:

- ❖ *High Cycle Fatigue / Low Cycle Fatigue Interaction.* Most of the effort performed under HCF/LCF Interaction has been in developing an understanding of baseline material behavior for

establishing the effects of other damage mechanisms. The many accomplishments in this area are described below:

- High resolution studies of LCF/HCF crack growth with the SwRI DISMAP system found no significant, systematic effect of periodic LCF unloads on near-threshold fatigue crack growth rates under high-R HCF cycling. This result is consistent with detailed crack-tip micromechanics analyses conducted under another program, which found no significant changes in crack-tip strains or crack closure with the periodic LCF unloads.
- The fatigue crack growth behavior of microstructurally short cracks, which have been known to propagate below conventional long-crack  $\Delta K_{th}$  values, was evaluated. Naturally-initiated fatigue cracks in smooth specimens (tested at  $\Delta\sigma = 80$  ksi,  $R = 0.1$ , and frequency 60 Hz) were documented via surface replication performed at uniform intervals of 15,000 cycles.

According to the general trend observed in Figure 18, an initially high crack propagation rate abruptly decreases, reaches certain minimum value, and then gradually increases. This is accompanied by substantial reduction in experimentally observed scatter in crack propagation rate as the crack grows. In Figure 18a, crack size corresponding to the minimum crack propagation rate is also compared to the average primary-alpha grain size. The major trend in crack propagation behavior changes from deceleration to acceleration after the crack tip passes through the first or second primary-alpha grain boundary. At the same time, in one case (specimen 2) an additional crack growth retardation event occurred when the crack size (depth or surface half-length) was five times larger than the average primary-alpha grain. Based on the data presented in Figure 18a, fatigue crack propagation behavior in the present material was divided into two separate regimes with respect to microstructural sensitivity.

Similar trends in fatigue crack propagation behavior can be seen in Figure 18b. In this graph, the results obtained are plotted as a function of stress intensity factor range,  $\Delta K$ , and compared to the crack propagation behavior of “long” cracks in both compact tension and surface flow type specimens. It can be seen that naturally-initiated “small” cracks propagate well below the “long” crack threshold, and that naturally-initiated “small” cracks propagate much faster than “long” cracks for stress intensity range values slightly greater than the “long” crack threshold. The tendency for faster propagation persists up to  $\Delta K \sim 10$  at which point both sets of data merge together.

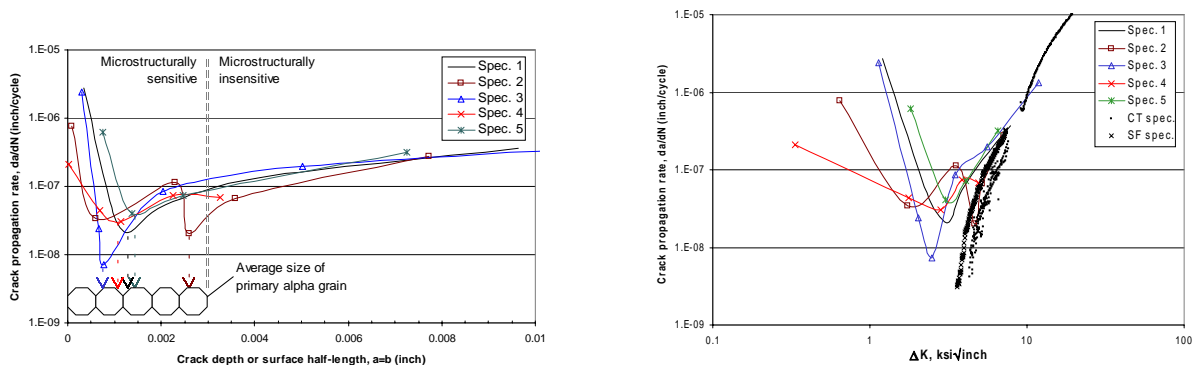
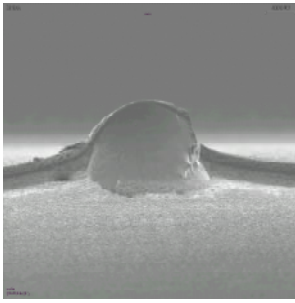


**FIGURE 18.** Fatigue Crack Propagation Rate of Naturally-Initiated “Small” Cracks as a Function of: (A) Crack Size and (B) Stress Intensity Factor Range.

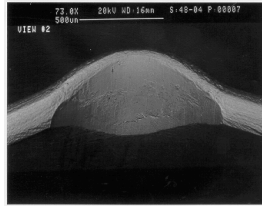
❖ **Foreign Object Damage.** Specific areas of progress are:

- Two geometries were selected for notched testing to estimate the effect of stress gradients and notch volume on initiation life. Each sample was designed to have a nominal  $K_t$  of 2.5. The test geometries included both flat notched specimens as well as the unnotched and machined notched tests of winged FOD specimens. All specimens were stress relieved and chem milled. Both stress-invariant and critical plane methods of modeling fatigue life were evaluated. During this evaluation, it became readily apparent that the specimens with small stressed areas had greater HCF capability (higher Walker equivalent stress prior to failure) than the smooth test data. This was especially true for the machined notch FOD test that had the smallest notch length (less than 0.015 inch). It was concluded that this behavior is best modeled by considering the size of the stressed surface area. This was treated quantitatively with the Weibull modified equivalent stress method. A stressed area weighting term was employed for a given specimen geometry and loading condition. Test results indicate that the presence of a large stressed area (unnotched FOD specimen) results in a predicted life similar to those of smooth specimens with a similarly highly stressed area. Yet, a relatively small notch (notched FOD specimens) can result in increased stresses prior to failure if the small area of highly stressed material is not accounted for in the analysis. The Socie stress model seems to correlate the notched data quite well, suggesting that the shear cracking mode might be dominant in the notched specimens. However, use of the Socie stress parameter along with the notch stress state (after accounting for notch-cyclic plasticity) does not adequately correlate with the smooth-data curve-fit. Further development is needed to account for possible material volume effects in notched specimens to allow correlation of smooth and notched data.
- FOD testing was performed on airfoil-shaped tension specimens and winged specimens. Three methods were used to simulate FOD in the winged specimens: machined notches with a 0.021-inch radius, ballistic ball impacts with 0.020 and 0.039-inch radius glass beads, and solenoid gun impacts with a chisel-point indenter (0.005 and 0.025-inch radii tips). Specimens were machined or impacted to simulate FOD nicks at 0° and 30° relative to the centerline of the leading edge region on the specimen. Low damage and high damage target levels were set at depths of 0.005 and 0.020-inch. Figure 19 compares 30° notches in sharp leading edge specimens with ballistic and solenoid gun impacts. Actual notch depths ranged from 0.003 to 0.009-inch and 0.015 to 0.026-inch.

Ballistic Impact with  
0.020 Inch Radius Ball



Solenoid Gun with 0.025  
Inch Radius Indentor



Solenoid Gun with 0.005  
Inch Radius Indentor

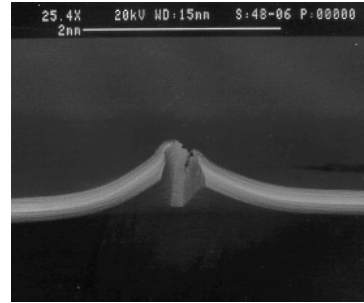


**FIGURE 19.** Representative FOD from Ballistic and Solenoid Gun Impacts (Sharp Leading Edge Specimens, 30° Impacts, High Damage Levels)

Results from endurance limit testing ( $10^6$  cycles) indicate that the ballistic impact results are not significantly different from the solenoid gun results at equivalent damage depths and impactor radii. The solenoid gun has since been adopted as the simulated FOD impactor of choice for its repeatability.

The airfoil-shaped specimen is based on the Air Force's diamond-like cross-section tension (DCT) specimen. Single FOD impacts were introduced to each specimen side, resulting in two FOD notches per specimen. The indentation from the FOD event was measured using an MTS deflectometer. The non-recoverable energy associated with the FOD impacts was recorded. While some of the results appear to show good repeatability, other results show significantly different energy levels for the same depth of FOD. Additional work is required before this method can be used to calibrate the level of FOD damage imparted to specimens.

Several un-impacted and impacted specimens were tested under axial-load-control HCF conditions for comparison to baseline smooth bar fatigue data. Figure 20 compares the  $R = -1$  and 0.5 diamond cross-section tensile (DCT or airfoil) test data with the smooth-bar baseline data. The data clearly show good agreement with smooth-bar baseline for non-impacted tests, and the negative effect that FOD has on HCF life. The non-recoverable energy showed poor correlation between the energy recorded and the subsequent HCF life of impacted specimens. Additional work is needed to better understand the effect of this parameter and technique. Fractography showed that some of the initiation sites were significantly (e.g., 0.004-inch) below the surface of the FOD impact. From the microstructural deformation observed below the FOD impact, it appears that significant cold work stresses should exist. However, these residual stresses were not measured.

❖ **Fretting Fatigue.** Specific areas of progress are:

- Multiaxial fatigue tests were performed on solid-round specimens for Ti-6Al-4V. All specimens were stress relieved and chem milled. Tests for torsion, proportional tension-torsion, and non-proportional tension-torsion were evaluated for cases where cyclic plasticity was not an issue and elastic-plastic finite element results were available. The Walker equivalent stress method was evaluated for predicting mean stress effects under uniaxial and multiaxial stress states for both smooth and notched fatigue specimens. The equivalent stress method is a stress invariant method that can be implemented into computationally efficient crack initiation codes such as NASALIFE. A variety of stress invariant multiaxial parameters were evaluated.

The stress invariant model that best predicted the experimental results is based on the effective stress range and a modified Manson-McKnight mean stress. Three different critical plane models, the Smith-Watson-Topper (SWT), the Fatemi and Socie (FS), and the Socie models were also evaluated. The SWT model was found to correlate the data with various stress-ratios quite well. The Socie effective stress parameter was able to collapse all of the data for the different R-conditions reasonably well in both the LCF and HCF regimes. The good correlation of the HCF data using the Socie model also suggests that a shear-cracking mode might be dominant in the HCF regime in general. The FS strain did not correlate the data as well as the Socie stress parameter. Further development is needed to better correlate data at different values of R using the critical plane methods.

- Friction experiments were conducted by Purdue University to study the evolution of the coefficient of friction,  $\mu$ , with the number of cycles in partial slip experiments in bare Ti-6-4 on Ti-6-4. The pads used were cylindrical, resulting in Hertzian distribution in the contact zone. Loading was stopped after running for a specified number of cycles. Then, without disturbing the pad/specimen contact, a waveform of increasing amplitude was applied to the specimen. The experiment was then stopped when the pad just started sliding (about 50 cycles). The average coefficient of friction was then calculated using the maximum value of the tangential force before the pad started sliding. The friction experiments were conducted with two different sets of pads of radii 5 inches and 7 inches. The maximum bulk stress applied during the experiments was 42 ksi. Figure 20 shows the results of the friction experiments. These results are similar to the results of fretting tests with flat pads performed at GEAE.

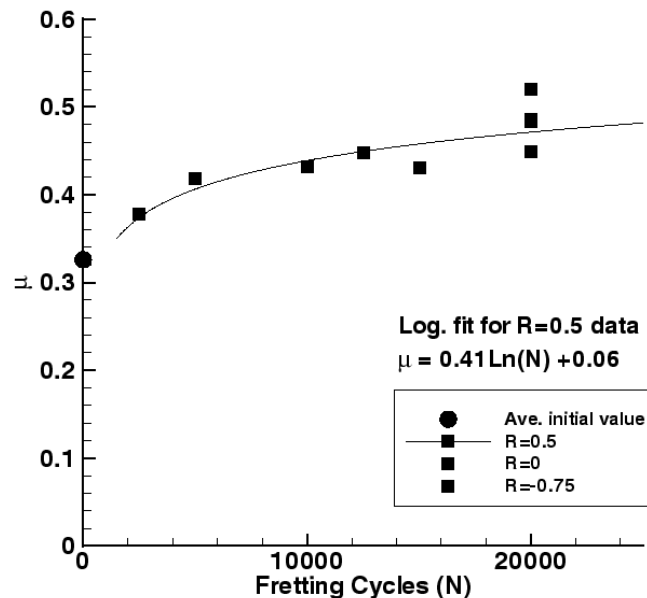


**FIGURE 20.** Evolution of Coefficient of Friction

- An investigation utilizing both integral equation and finite element methods (FEM) was performed to determine edge-of-contact stresses. The singular integral equation approach is based on the solution representing two-dimensional, plane-strain elastic contact of similar materials with an arbitrary surface profile. The integral equations can be derived from classical theory of elasticity results relating the slope of the contacting surfaces to the resulting

interfacial tractions. The boundary conditions for this type of problem are the force and moment equilibrium conditions. In addition, the pressure vanishes at the ends of the pad. The singular integral equation can then be solved using trigonometric variable transformations. The surface normal traction can be obtained from any arbitrarily specified surface profile, normal load, and bending moment. Once the surface tractions are evaluated by this procedure, sub-surface stresses can be obtained using discrete Fourier transformation techniques.

The local edges of contact stresses were also obtained using FEM. However, FEM requires a very fine mesh in order to obtain a fully converged solution. Stress analyses were performed for a relatively simple two-dimensional problem. A mesh size of 0.0625 mil was required to obtain a fully converged solution. Meshing to this level for a complex three-dimensional skewed disk-airfoil attachment would be a very computationally intense problem and is not well suited to an engineering or design environment. For the two-dimensional experiments in the current program, the singular integral equations give a solution that matches very well with the solution obtained from the finite element analysis as shown in Figure 21.

**Pressure and Shear under a Mindlin Loading Scheme**

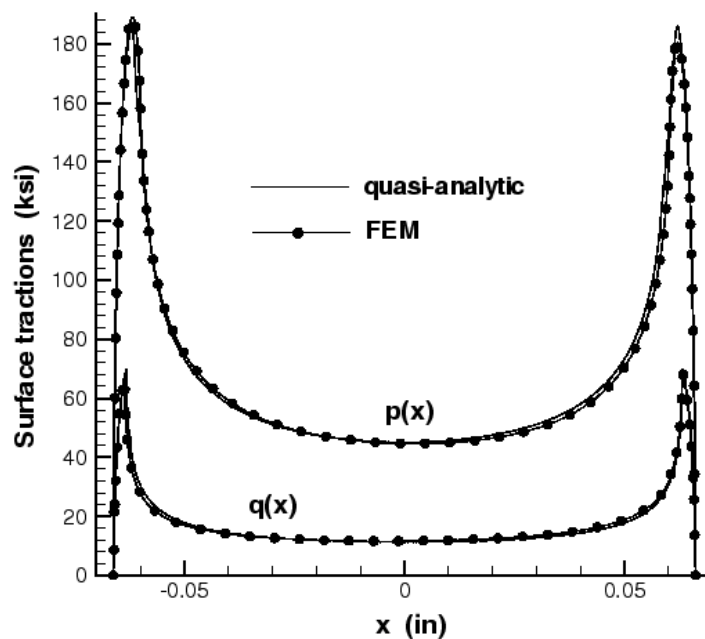


**FIGURE 21.** Comparison of Surface Normal Tractions Obtained from Integral Equation and FEM Methods

- ❖ **Damage Tolerant Life Prediction Methodologies:** Damage tolerant life prediction methodologies have been developed or utilized as mentioned in the three damage state areas above. In each of the three areas, exit criteria have been developed to ascertain the level of accuracy of the techniques for determining the HCF alternating load capability of damaged materials. The metric for assessing the predictive accuracy is based on the ratio of “actual to predicted” capability where actual capability is determined in bench testing. For the different damage states, exit criteria are based on different limits put on the mean and coefficient of variation (COV) of the “actual-to-predicted” capability, as compared to that for baseline smooth axial fatigue specimens. The exit criteria are listed in Figure 22.

<u>Damage State</u>	<u>Mean Ratio*</u>	<u>COV*</u>
LCF/HCF Interaction	0.95 – 1.05	1.25 X
Foreign Object Damage	0.85 – 1.15	2.50 X
Fretting Fatigue	0.85 – 1.15	2.50 X

\* compared to baseline smooth axial fatigue specimens

**FIGURE 22. Materials Damage Tolerance Damage State Exit Criteria**

**Participating Organizations:** University of Dayton Research Institute, General Electric Aircraft Engines, Pratt & Whitney, Rolls Royce Allison, Honeywell Engines and Systems, Southwest Research Institute, Purdue University, North Dakota State University, and the University of Illinois.

**Points of Contact:**

Government

Dr. Theodore Nicholas  
U.S. Air Force  
AFRL/MLLN, Bldg. 655  
2230 Tenth St., Suite 1  
WPAFB, OH 45433-7817  
Phone: (937) 255-1347  
Fax: (937) 656-4840  
Email:  
Theodore.Nicholas@afrl.af.mil

Government

Mr. Joseph G. Burns  
U.S. Air Force  
AFRL/MLLN, Bldg. 655  
2230 Tenth St., Suite 1  
WPAFB, OH 45433-7817  
Phone: (937) 255-1360  
Fax: (937) 656-4840  
Email: Joseph.Burns@afrl.af.mil

Contractor

Dr. Joseph P. Gallagher  
Univ. of Dayton Research Institute  
300 College Park  
Dayton, OH 45469  
Phone: (937) 229-2349  
Fax: (937) 229-3712  
Email: gallagher@udri.udayton.edu

## **2.5 Advanced HCF Life Assurance Methodologies (Fan & Turbine)**

*FY 99-02*

**Background:** This program is a follow-on effort to Effort 2.4, “Improved HCF Life Prediction,” and is focused on the extension and validation of the technologies developed in the earlier effort to other titanium alloys for use in the fan section, as well as to single crystal nickel-base superalloys for use in the turbine section. The objectives of this program are: (1) to extend the understanding of damage mechanisms in  $\alpha+\beta$  processed Ti-6Al-4V blades and disks to other titanium alloys with varying microstructures, (2) to develop a better understanding of the underlying damage mechanisms to which single crystal nickel-base superalloy blades and disks are subjected, and (3) to extend and validate the damage tolerant life prediction and design methodologies developed for  $\alpha+\beta$  processed Ti-6Al-4V to other titanium alloys and to single crystal nickel-base superalloys.

A comprehensive database of test results are being developed to describe all aspects of material HCF behavior for  $\beta$ -processed Ti-17 titanium and PWA 1484 single-crystal nickel-base superalloy. The damage states that increase the potential for HCF failures will then be defined. Finally, improved test methods, improved analytical approaches, and total life prediction software for titanium and single crystal superalloy, will be developed.

**Recent Progress:** This work has recently started and limited testing has been performed. No results are available at this time.

**Participating Organizations:** Air Force Research Laboratory (AFRL), Air Force Office of Scientific Research (AFOSR), University of Dayton Research Institute, General Electric Aircraft Engines, Pratt & Whitney, Rolls

Royce Allison, Honeywell Engines and Systems, Southwest Research Institute, Purdue University, University of Illinois, North Dakota State University, Rensselaer Polytechnic Institute.

**Points of Contact:**

Government

Maj Brian Sanders, Ph.D.  
U.S. Air Force, AFOSR/NA  
110 Duncan Avenue, Suite B115  
Bolling AFB, DC 20332-0001  
Phone: (202) 767-6063  
Fax: (202) 767-4988  
Email: brian.sanders@afosr.af.mil

Government

Mr. Joseph G. Burns  
U.S. Air Force  
AFRL/MLLN, Bldg. 655  
2230 Tenth St., Suite 1  
WPAFB, OH 45433-7817  
Phone: (937) 255-1360  
Fax: (937) 656-4840  
Email: joseph.burns@afrl.af.mil

Contractor

Dr. Joseph P. Gallagher  
Univ. of Dayton Research Institute  
300 College Park  
Dayton, OH 45469  
Phone: (937) 229-2349  
Fax: (937) 229-3712  
Email: gallagher@udri.udayton.edu

## 2.6 Conclusion

The Materials Damage Tolerance Action Team dramatically increased the propulsion community understanding associated with and contributing to turbine engine high cycle fatigue. Specifically, this Team developed a new titanium Foreign Object Damage (FOD) life model: a new FOD baseline for HCF analysis with increased understanding of FOD occurrence, locations and severity. The Materials Team also developed a unique HCF bench test that can simulate both fretting fatigue and contact stresses and improve overall HCF predictive capability, and developed new methods for modeling fretting fatigue life, crack growth in fretting fatigue, and contact stresses. A low cycle / high cycle fatigue interaction model is also being formulated. Currently, fretting of blades is the most difficult failure mode, as there is significant disagreement between predicted and observed data. An effort addressing single crystal blades is also currently underway.